Blue - and Green-Light-Induced Reductions and *C-C* Bond Formations with TiO_2 and $PbBiO_2X$

Dissertation

zur Erlangung des Doktorgrades der Naturwissenschaften
(Dr. rer. nat.)
an der naturwissenschaftlichen Fakultät IV
-Chemie und Pharmazie-
der Universität Regensburg

vorgelegt von
Stefan Füldner
aus Ludwigsfelde

November 2010

The experimental part of this work was carried out between September 2007 and October 2010 under the supervision of Prof. Dr. Burkhard König at the Institute of Organic Chemistry, University of Regensburg.

The PhD thesis was submitted on:		22th November 2010
The colloquium took place on:		17th December 2010
Board of Examiners:	Prof. Dr. M. Schütz	(Chairman)
	Prof. Dr. B. König	(1st Referee)
	Prof. Dr. O. Reiser	(2nd Referee)
	Prof. Dr. A. Pfitzner	(Examiner)

Danksagung

Meinen besonderen Dank möchte ich meinem Doktorvater Prof. Dr. Burkhard König für die Möglichkeit an einem zukunftsorientierten Thema zu arbeiten, für die schnellen Korrekturen sämtlicher Manuskripte und die stetigen Diskussionsbereitschaften entgegenbringen. Danke auch für die Eröffnung der Möglichkeiten hinsichtlich der Stipendien während meiner Promotionszeit und Motivationen in den gesamten Projekten, ohne die diese Arbeit nicht möglich gewesen wäre.

Ich danke den Vorsitzenden der *Bayerischen Eliteförderung* (Stipendium 04-2008 bis 03-2010) und des Graduiertenkolleges *Chemische Photokatalyse - GRK1626* (Stipendium 04-2010 bis 10-2010) für die finanziellen Unterstützungen.

Für die gute und sehr erfolgreiche Zusammenarbeit danke ich den Mitarbeitern Matthias Neumann und PD Dr. Kirsten Zeitler des Institutes für Organische Chemie im Projekt der enantioselektiven Photokatalyse; Dr. Patrick Pohla, Stephan Dankesreiter und Roland Stadler vom Institut für Anorganische Chemie vom Lehrstuhl von Herrn Prof. Dr. A. Pfitzner sowie ihm selbst im Projekt der photokatalytischen Reduktionen mit den Halbleitern $PbBiO_2X$; Dr. Michael Gruber von der Abteilung Anästhesie vom Universitätsklinikum Regensburg für sämtliche Wasserstoffmessungen; Heiko Ingo Siegmund und Dr. A.-J. Schroeder von der Abteilung Analytik vom Universitätsklinikum Regensburg für die wundervollen TEM-Aufnahmen; Dr. Rudolf Vasold aus unserer Arbeitsgruppe für die permanente Unterstützung in den GC- und GC-MS-Analytiken.

Meinen aktuellen und ehemaligen Laborkollegen danke ich für sämtliche Hilfen und für die Atmosphäre im Labor selbst. Christoph Harlander danke ich vor allem für seine nicht endende Neugier in seinem Masterprojekt, sein Durchhaltevermögen und noch viel mehr die wundervolle Freundschaft. Peter Raster sei auch hier für seine absolute Zuverlässigkeit und für all seine fachlichen und privaten Diskussionen gedankt, die so manche Perspektive eröffnet haben.
Den ehemaligen Mitarbeitern meines kleinen Arbeitskreises Alexandra Frimberger, Ralph Mild, Tobias Trottmann und Katharina Limm danke ich zunächst als ehemaliger Chef für ihre unermüdliche Schaffenskraft, ihr Vertrauen in meine Führungsqualitäten und als Freund unendlich dafür, dass es sie für mich gibt.

Meiner besten Freundin und Lieblingsprinzessin Saskia Graf möchte ich einen Dank entgegenbringen, den ich wohl nicht in Worte fassen kann: Zuhause war für mich immer da, wo Du warst. Danke für die unendlich tiefen Gespräche, das Tanzen, die vielen Motivationen, die kleinen Lichter in meinen dunkleren Zeiten, den gemeinsamen Titel *Mr. und Mrs. Falkenfelser 2008*, die Beachvolleyballabende und die ewig in Erinnerung bleibenden Geburtstagsparties. Meine Hochachtung gilt Dir als Wissenschaftlerin und Millionen Mal mehr als herzensguter Mensch.

Meinem wiedergefundenen Vater, Christiane und meinen Großeltern danke ich für ihre Unterstützungen und das größte Geschenk, was man sich zu Weihnachten 2009 wohl hätte vorstellen können.

Carolinchen danke ich für all Ihre unendliche Unterstützung, Ihre Geduld und Ihr Verständnis mit mir als schwierige Person in einer noch schwierigeren Zeit und für den großen Glauben an mich.

Dr. Boe Geun Kim und Dr. Katja Vorndran danke ich für das Erweitern meiner chemischen Grundlagen innerhalb meiner Ausbildung und meines Studiums, ohne die all das hier nicht möglich gewesen wäre.
Meinen *kleinen Chemikern* Hanna Bartling, Veronika Kropf, Malte Hansen, Michael Hammer, Kathrin Hajek und Mathias Schwedes danke ich für ihre Praktikumszeit bei mir, ohne die so manches Ergebnis nicht möglich gewesen wäre.

Drücke Euch allen für die Erfüllung Eurer Träume die Daumen.

For my refound father Gerd

and

my Lieblingsprinzessin

Sassi.

Zwei Dinge sind zu unserer Arbeit nötig:
Unermüdliche Ausdauer und die Bereitschaft,
etwas, in das man viel Zeit und Arbeit gesteckt hat,
wieder wegzuwerfen.

Albert Einstein

Julia Nistor „Photokalytisch“

August 2009

Acryl auf Hartfaser 120 x 90 cm

Table of Contents

Abbreviations

ΔG	change in free energy
DMSO	Dimethylsulfoxide
DMU	Dimethylurea
E	redox potential
GC	Gas Chromatography
GC/ MS	Gas Chromatography with Mass Spectrometry Detector
LED	Light Emitting Diode
h	hours
M	mol per liter
m	mass
MeCN	Acetonitrile
mL	milliliter
µL	microliter
MLCT	Metal to Ligand Charge Transfer
m.p.	melting point
NMR	Nuclear Magnetic Resonance
N3	*cis*-Diaquadithiocyanatobis(2,2'-bipyridyl-4,4'dicarboxylate)-ruthenium(II)
SCE	Saturated Calomel Electrode
t	time
TEM	Transmission Electron Microscopy
TEMPO	2,2,6,6-Tetramethyl-1-piperidinyloxy
THF	Tetrahydrofurane
TEOA	Triethanolamine
TiO_2	Titaniumdioxide
TMU	Tetramethylurea
TU	Thiourea
UV	Ultra Violet
Vis	Visible
z	number of charges

1 Green-Light Photocatalytic Reductions via Dye-sensitized TiO_2 and Transition Metal Nanoparticles or small Amounts of Urea Derivatives

1.1 Introduction

Following the prognoses of the WBGU (*Wissenschaftlicher Beirat der Bundesregierung, Globale Umweltveränderungen*) and the UN, an adequate energy supply is already limited by the use of conventional resources and a steady increase in population today. Biomass is investigated to satisfy human energy hunger, but too much space is needed if population is going to increase to 20 Billion people in 2050.[1] While energy secures humans survive, chemistry is the base for our comfort in life: (a) active agents in medicine, (b) textile industries, (c) automobiles, (d) communication and so on. While energy can be produced sustainable from wind, water power and sunlight, a direct conversion into chemically stored energy is only possible using sunlight. Photovoltaic systems for the conversion of solar energy into electrical power have already evolved into a wide range of applications.[2] Photocatalysts, which utilize light to drive chemical reactions,[3] are less developed and typical applications are the photodegradation of organic pollutants with TiO_2 and UV irradiation in waste water treatment[4] or self cleaning surfaces.[5] Large scale photocatalytic fuel generation,[6] e.g. by water splitting,[7] still lacks endurance and efficiency, but photocatalytic fine chemical synthesis has been achieved. Recent examples of homogeneous photocatalysis[8] include alkyne hydrogenation,[9] the direct asymmetric alkylation of aldehydes,[10] enantioselective cyclisation reactions[11] and methanol addition to glycals.[12] Homogeneous photocatalysis has the disadvantage of additional separation steps of products and catalysts after the reaction. Heterogeneous photocatalysts overcome this problem and especially TiO_2 fulfills several demands of a modern photocatalyst: (a) Visible light of the solar spectrum can be used by sensitizing the semiconductor surface with dyes absorbing above 400 nm, (b) immobilization on glass surfaces has been described and is used in Grätzels Cells[13] and (c) different photocatalytic reaction types have been described, such as oxidations or reductions.[14]

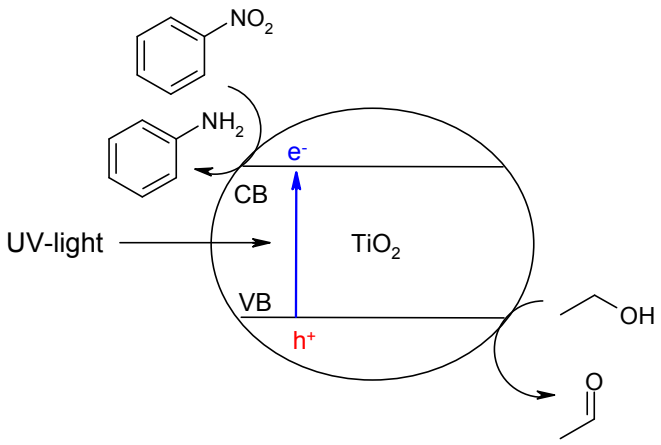

Scheme 1. TiO_2 based UV-induced reduction of nitrobenzene to aniline.

Semiconductors as cadmiumsulfide have been developed for the synthesis of unsaturated α-cyano-homoallyl amines from imines and olefins,[15] but remain one of a few applications in organic synthesis. In addition, metal complexes[16] and metals[17] are deposited on TiO_2 to increase its photocatalytic efficiency.[18] A recent example of the application of sensitized TiO_2 photocatalysis to organic synthesis is the TEMPO mediated aerobic oxidation of alcohols using blue light irradiation and oxygen,[14] whereas non-modified TiO_2 was used to mediate the oxidative addition of THF to quinolines[12] or the reduction of nitrobenzenes with UV light[19] (Scheme 1).

Here, we report a method for selective reductions of nitro arenes with blue and green light without complicate and expensive modification or preparation of the TiO_2 particles. Our simple, but effective heterogeneous photocatalysts are derived from commercially Degussa P25 TiO_2, ruthenium complex **N3** and added trace amounts of metal salts or urea derivatives. The catalyst preparation is achieved by simple mixing and does not require any special procedures. Samples were irradiated with High Power LEDs 440 nm or 530 nm / ± 10 nm. The photoconversions of organic substrates are very clean, as verified by gas chromatography monitoring and in many cases quantitative.

1.2 Transition Metal Nanoparticles

1.2.1 Results and Discussions

Irradiation of unmodified TiO_2 at 530 nm lead to low conversions of nitrobenzene of about 2 % (Table 1, entry 2). TiO_2 modified with **N3**, but no deposited transition metal ions gave conversions of nitrobenzene to aniline of 39 % (table 1, entry 3). No conversion was detected without green light irradiation or by irradiating **N3** without TiO_2 (Table 1, entry 1).

Table 1. Metal amount-conversion dependency of the photo reduction of nitrobenzene to aniline.

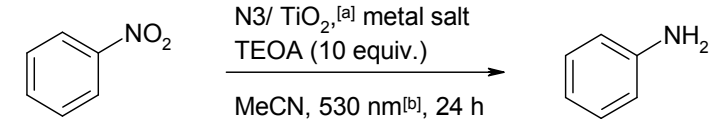

2 x 10^{-4} mol

Entry	Added Metal Salt [mol%]	No Added Metal Salt	Nitrobenzene Conversion [%][c]						
			Pt^{4+}	Pt^{2+}	$Pt^{(0)}$[g]	$Pt^{(0)}$[h]	Pd^{2+}	Ag^{+}	Au^{3+}
1[d]	0	0							
2[e]	0	2							
3[f]	0	39							
4	0.000001		37	46	46	> 99	50	46	44
5	0.00001		27	39	32	> 99	39	29	32
6	0.0001		51	90	49	99	49	49	> 99
7	0.001		51	41	49	> 99	40	39	83
8	0.01		43	> 99	28	> 99	> 99	59	85
9	0.1		67	> 99	39	72	> 99	65	> 99
10	0.5		38	36	32	40	> 99	30	49
11	1.75		25	27	26	23	56	7	12
12	0.1		-	99(91)[k]	-	-	99(93)[k]	-	-
13	0.001		-	-	-	-	-	-	99(92)[k]

[a] 50 mg TiO_2 with immobilized N3 (2 mol%). [b] 3 Watt electrical power. [c] Integration of signals in GC chromatograms. [d] 50 mg TiO_2 with 0.01 mol% K_2PtCl_6 in the dark. [e] 50 mg TiO_2 without immobilized N3 and with transition metal. [g] 50 mg TiO_2 without immobilized N3 and without transition metal. [g] Particles synthesized by reduction with $NaBH_4$ and mercaptosuccinic acid.[20] [h] Particles synthesized by reduction with UV-light < 300 nm. [i] 2 x 10^{-3} mol nitrobenzene, 36 h irradiation time. [k] Isolated aniline yields after distillations are given in brackets.

The addition of small amounts of transitions metal ions to the reaction mixture lead to a significant enhancement of the photocatalytic activity: 67 % conversion for 0.1 mol% and 51 % for 0.001 mol% K_2PtCl_6 (table 1, entries 7, 8 and 9). Quantitative conversions of nitrobenzene to aniline were observed with 0.1 mol% of Pt(II) or even smaller amounts of Pd(II) salts. A similar effect in non-sensitized reactions has been previously reported for silver clusters deposited on TiO_2.[16] The systematic variation of the transition metals, their amounts and the method of their reduction revealed a dependency between the nature of the metal and the optimal catalytic amount (Table 1): Quantitative conversions > 99 % are observed for 0.5 - 0.01 mol% using Pt(II) and Pd(II), while reduced Pt(IV) and Ag(I) salts did not lead to complete conversions under the experimental conditions with best results of 67 % for 0.1 mol% Pt(IV) and 65 % for 0.1 mol% Ag(I).

The photocatalytic activity of the Pt(0) species depended on their preparation: The reduction of Pt(IV) and stabilization of the colloid by mercaptosuccinic acid yielded less active catalysts. On the other hand, photochemically prepared Pt-colloids showed quantitative conversion of nitrobenzene to aniline in a range of 10^{-1} - 10^{-6} mol% (Table 1, entries 4 - 8). The photocatalytic activity depended on the oxidation state of the platinum source, which was either Pt(IV), Pt(II) or Pt(0). This has been observed earlier by Remita et al. in photo-degradations by platinum-doped TiO_2: Under visible light irradiation the photodegradation activities followed the order Pt-cluster > Pt(II) >> Pt(IV) and was explained by the ability of the Pt-clusters to act as weak temporary electron scavengers.[21] Using Au(III) salts leads to quantitative conversions at 10^{-1} and 10^{-4} mol%. For every metal salt an optimum amount range was found. They are all below 1 mol%, some are as low as 10^{-4} mol%. Amounts higher than 1 mol% decreased the catalytic activity. Ozin et al. recently reported that the size distribution of deposited platinum clusters on TiO_2 depends on the platinum loading and the photocatalytic activity of the material in photodecomposition increased beyond a critical cluster size of 2 nm.[22] TEM pictures from our reaction solutions with the optimum catalytic amounts for Pt(II), Pd(II) in 10^{-2} mol% and Au(III) in 10^{-4} mol% showed a similar morphology for each of the resulting particles (Figure 2). No transition metal particles were found on the surface of TiO_2. This indicates that (a) a specific amount for every transition metal is needed to get the optimum particle size for the photocatalytic reduction under these conditions and (b) the active catalyst is prepared heterogeneously, but the reduction reaction is homogeneous mediated by nanometer size metal clusters.

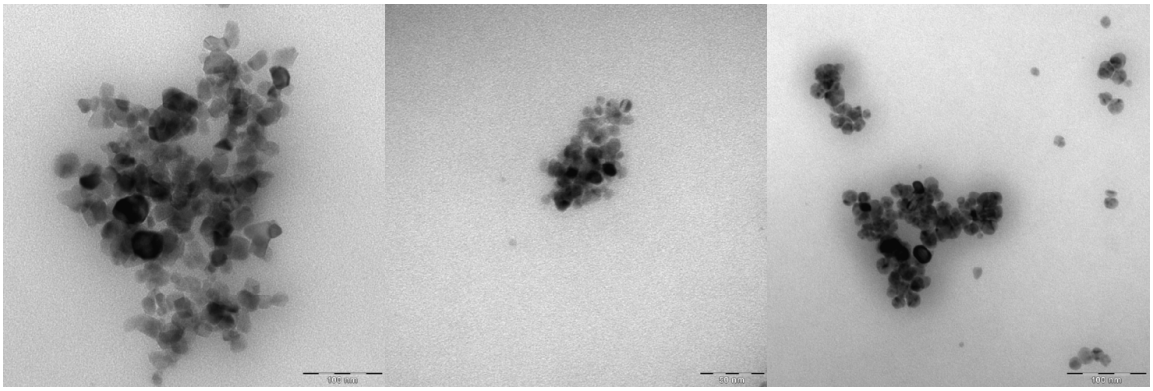

Figure 1. TEM-pictures of nanoparticles found in solution after the photocatalytic reduction (left) 0.01 mol% Pt(II), (middle) 0.01 mol% Pd(II) and (right) 0.0001 mol% Au(III).

The reactions in Table 1 correspond to minimum turnover numbers of 1000 for Pt(II) (0.1 mol%), 9996 for Pd(II) (0.01 mol%) and 995900 for Au(III) (10^{-4} mol%). The selective green light irradiation required longer irradiation times for complete conversion if compared to UV experiments, however, no side products of the reduction were detected when analyzing the samples by GC and GC-MS. A quantum efficiency of 8 % was determined for the reduction reaction under the optimized conditions. To demonstrate the use of the green light photo reduction on laboratory preparative scale, 2 x 10^{-3} mol of nitrobenzene were reduced and the product was isolated by distillation (Table 1, entries 12 and 13). Quantitative conversions and high yields were obtained for 0.1 mol% added Pd^{2+} and Pt^{2+} and for 0.0001 mol% of Au^{3+} when irradiating the samples for 36 h. As the composition of the catalyst system is similar to reported hydrogen generating photocatalysts, consisting in the simplest case of a ruthenium complex, an electron mediator and colloidal palladium, hydrogen was suspected as an intermediate and the chemical reduction reagent. Gas chromatographic analyses of the head space of a reaction sample using the conditions of entry 9, table 1 for 0.1 mol% Pd^{2+}, clearly showed the presence of 6 % hydrogen gas after 10 h of irradiation. The role of the metal clusters in this catalytic system could be twofold: They accept electrons from the conduction band of the TiO_2 and generate dihydrogen by reduction of protons provided by the TEOA,[23] but they also catalyze the hydrogenation of the organic substrate. Monitoring of the photo reduction (Figure 2) showed an induction period of the reaction of about 8 - 12 h while full conversion of nitrobenzene to aniline without any transition metal has been observed when irradiating the sample for 48 hours. A likely explanation for this observation could be the necessary formation of the reduced metal clusters and the buildup of a hydrogen gas pressure before an effective substrate conversion starts.

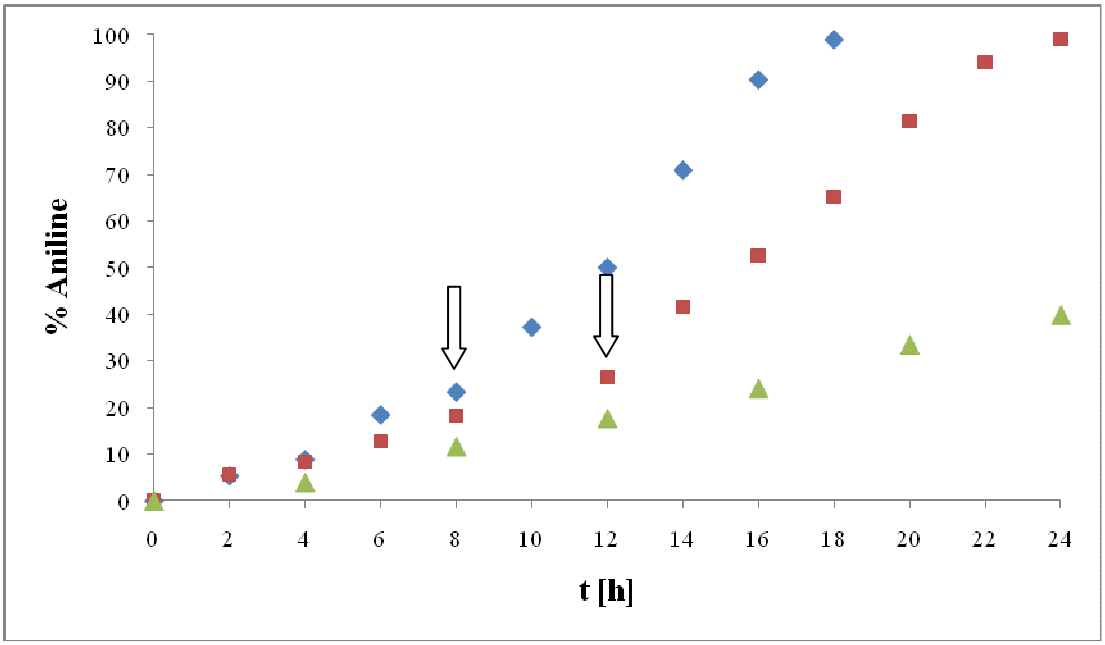

Figure 2. Time dependent conversion of nitrobenzene to aniline with 0.01 mol% Pd(II) (red spots), 0.0001 mol% Au(III) (blue spots) and without transition metal catalyst (green spots).

After optimization of the reaction conditions the substrate scope was investigated. Tables 2a and b summarize the results for standard reaction conditions of 24 h irradiation at room temperature. Ethyl 4-nitro benzoate, 4-nitro benzonitril, 4-nitro benzaldehyde and 4-bromo nitrobenzene are reduced to the corresponding anilines, wherein smaller amounts of added K_2PtCl_6 gave better conversions under the experimental conditions. No reduction of the aldehyde functional group is observed. In the case of 4-bromo nitrobenzene dehalogenation occurs as a competing process at high platinum concentrations. No other side products were detected by GC analysis for the photo reductions. 4-Nitro phenol is not reduced under the experimental conditions and 1,4-dinitrobenzene gives nitro aniline, but only in small yields.[24] In contrast, 1,2-dinitrobenzene is reduced to 2-nitro aniline in good yields with small amounts of the corresponding nitro hydroxylamine as a side product (Table 2b, entry 1). 2-Nitro benzaldehyde and 2-nitro acetophenone are reduced to the corresponding anilines. However, depending on the amount of platinum salt added the corresponding 1,2-benzisoxazole becomes the major product. The preparation of 1,2-benzisoxazoles has been described previously using 2 - 5 equivalents of indium as reduction reagent.[25] As expected, the conversion of benzaldehyde to benzyl alcohol is low under the experimental conditions.

Table 2a. Green-light induced reductions of nitrobenzene derivatives.

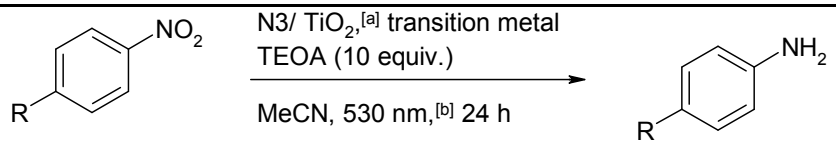

R = CO_2Et, CN, CHO, Br, NO_2

Starting Material	2 x 10^{-4} mol K_2PtCl_6 [mol%]	Products [%][c]		
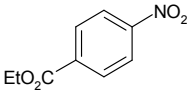	0.0001	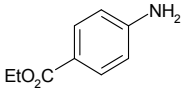	**89**	
	0.001		79	
	0.01		69	
	0.5		87	
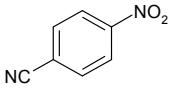	0.0001	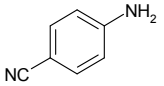	58	
	0.001		**85**	
	0.01		60	
	0.5		59	
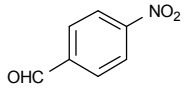	0.0001	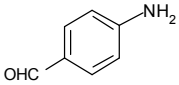	76	
	0.001		**89**	
	0.01		85	
	0.5		63	
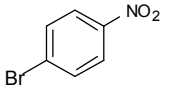	0.0001	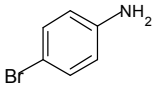	**84**	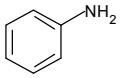
	0.001		49	
	0.01		48	
	0.5		23	
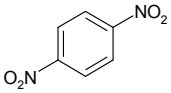	0.0001	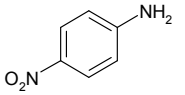	21	
	0.001		20	
	0.01		**24**	
	0.5		21	

	-
	6
	-
	64

[a] 50 mg TiO_2 with immobilized N3 (2 mol%). [b] 3 Watt electrical power. [c] Integration of signals in GC chromatograms.

However, pyridine-4-carbaldehyde is reduced to the corresponding benzyl alcohol in up to 80 % while aliphatic aldehydes are not reduced at all. This effect might be explained by the necessity of an electron poor aromatic system for an electron scavenging before the aldehyde is reduced. Pyridine is known as an electron poor aromatic system compared to benzene. The reduction of stilbene to 1,2-diphenylethane is possible under these reaction conditions, but the conversions remain incomplete within 24 h.

Table 2b. Photocatalytic reduction of *o*-substituted nitrobenzenes, benzaldehydes and stilbene.

Starting Material[a]	K_2PtCl_6 [mol%]	Products [%][b]			
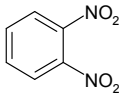	0.0001	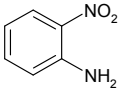	75	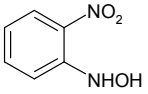	22
	0.001		91		9
	0.01		85		15
	0.5		88		12
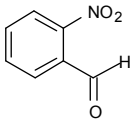	0.0001	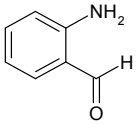	15	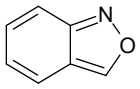	29
	0.001		26		62
	0.01		18		62
	0.5		22		71
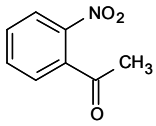	0.0001	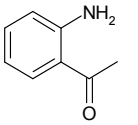	66	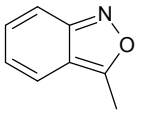	33
	0.001		66		33
	0.01		79		21
	0.5		79		20
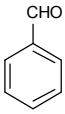	0.0001	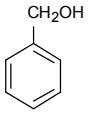	6		
	0.001		12		
	0.01		7		
	0.5		7		
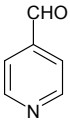	0.0001	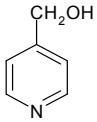	80		
	0.001		73		
	0.01		78		
	0.5		76		
	0.0001		36		
	0.001		44		
	0.01		33		
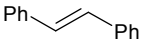	0.5	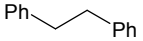	40		

[a] Standard conditions as described in table 2a. [b] Integration of signals in GC chromatograms, qualitative analysis via GC-MS.

We suppose the following mechanism because of these reasons: (a) Only nitrobenzenes and stilbene is reduced, (b) Hydrogen has been detected and (c) Transition metal clusters have been found in solution (Scheme 2).

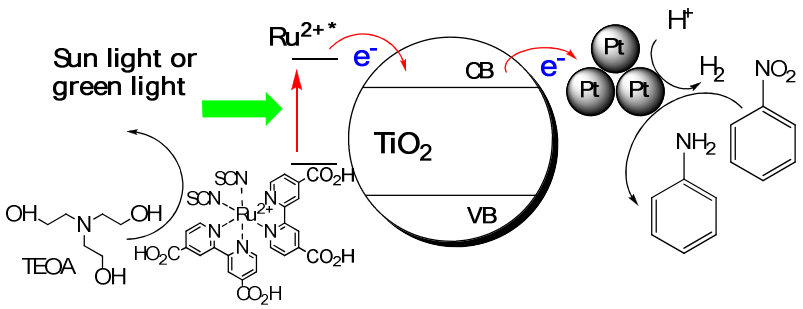

Scheme 2. Supposed mechanism of the green-light-induced reductions of nitrobenzenes via dye-sensitized TiO_2 and transition metal nanoparticles.

The dye **N3** is excited by green light from LEDs or sun light, the excited electrons are injected into the conduction band of TiO_2, transition metal ions take up these electrons, are reduced to their metals and form clusters in solution. Hydrogen is produced at these clusters from the acidic protons of TEOA and reduce nitrobenzene derivatives to their anilines. The catalytic circle is closed by the re-reduction of the oxidized dye by TEOA.

The photocatalyst system absorbs in the most intensive region of the solar spectrum and is therefore suitable to work in sun light. Photocatalytic reduction reactions using the standard apparatus and a **N3**/TiO_2/K_2PtCl_6 photocatalyst were performed at different weather conditions with daylight and sun irradiation (late summer, south of Germany). Table 3 summarizes the results. On a rainy and overcast day the conversion in nitrobenzene reduction is, as expected, only small. However, with increasing sunshine the nitrobenzene conversion reached 80 % and maximal TON, with respect to the added platinum catalyst, of more than 67000 after 11 hours which is due to the stronger intensity of green and UV light. Using a UV cut off filter (< 450 nm) conversion of the nitrobenzene reduction decreased to 67 % in 11 hours for 0.1 mol% Pt(IV) which underlines the role of UV-light in this photo process.

Table 3. Reduction of nitrobenzene to aniline using sunlight and **N3**/TiO_2/K_2PtCl_6 photocatalyst.

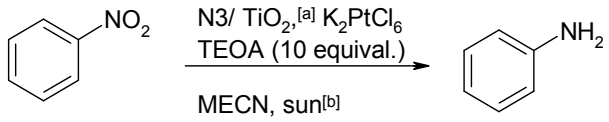

2×10^{-4} mol

Weather	Temp. [°C]	Platinum Catalyst [mol%]	Irradiation Time [h]	Nitrobenzene Conversion [%][c]	TON with respect to Pt
	15	0.1	11	4	40
	15	0.001	11	5	5000
	20	0.1	11	15	150
	20	0.001	11	11	11000
	35	0.1	11	80	800
	35	0.001	11	67	67000

[a] 50 mg TiO_2 with immobilized N3 (2 mol%). [b] Direct sunlight. [c] Integration of signals in GC chromatograms.

The oxidations of alcohols as methanol, ethanol or *p*-methoxybenzyl alcohol have been investigated to find a productive sacrificial redox reaction, but no reduction of nitrobenzene and no oxidation of the alcohols have been observed. This is in agreement with the redox potentials of the complex **N3**[44] and the investigated alcohols:[17] with $E(Ru^{3+}/Ru^{2+})$ = -0.85 V and $E(EtOH/CH_3CHO)$ = 1.25 V a valule of ΔG = 30.6 kJ/ mol is calculated clearly indicating that an electron transfer from the alcohol to the ruthenium complex **N3** is thermodynamically not possible.

1.2.2 Conclusion

The combination of ruthenium dye-sensitized TiO_2, as used in the photovoltaic Graetzel cell, with *in situ* generated transition metal nanoparticles of a size in the order of 10 to 20 nm leads to photo reduction catalysts that work with green light irradiation. The catalysts are simple to prepare and apply, and allow the complete, selective and clean conversion of nitrobenzene derivatives to the corresponding anilines. The use of green light irradiation of low energy avoids the formation of unwanted side products and rapid catalyst decomposition. Optimization studies revealed the amount of initially added transition metal salts as critical for an effective catalysis, as it determines the size of the *in situ* formed nanoparticles. Their activity as hydrogen evolution and hydrogenation catalysts is size dependent, as known from other studies.

The described photocatalyst may find applications in synthesis, as the metal salts exhibit some selectivity in the reduction reaction and conversions can be performed using energy efficient green light high power LED or direct sun light.

1.3 Urea and Derivatives

1.3.1 Results and Discussions

Thiourea has been widely described as catalyst in alcohol photooxidations,[8] asymmetric hydrogenation of nitroalkenes[26] or for asymmetric Morita-Baylis-Hilman reactions[27], but not in blanc or dye-sensitized TiO_2 catalysis. Organic electron mediators as urea and derivatives or DMSO would be an improvement towards sustainability compared to the transition metals, too,[28] because they are less expensive and show smaller environmental toxicity. Therefore, urea, DMU, TMU, thiourea and DMSO have been investigated towards their catalytic role within the dye-sensitized TiO_2 system (Table 4).

Table 4. Catalyst amount-conversion dependency of the photoreduction of nitrobenzene to aniline.

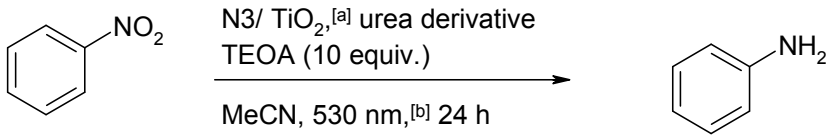

2 x 10^{-4} mol

Entry	Added Catalyst Amount [mol%]	Nitrobenzene Conversion [%][c] No Added Catalyst	Urea	DMU	TMU	thiourea	DMSO
1[d]	0	0					
2[e]	0	0					
3[f]	0	39					
4	0.000001		> 99	> 99	83	90	94
5	0.00001		79	51	72	51	93
6	0.0001		> 99	> 99	95	> 99	48
7	0.001		49	86	78	> 99	54
8	0.01		80	> 99	91	> 99	27
9	0.1		55	49	78	75	30
10	1.75		54	49	47	41	48
11	10		69	73	43	51	53

[a] 50 mg TiO_2 with immobilized N3 (2 mol%). [b] 3 Watt electrical power. [c] Integration of signals in GC chromatograms. [d] 50 mg TiO_2 with 0.0001 mol% urea in the dark. [e] 50 mg TiO_2 without immobilized N3 and with urea. [f] 50 mg TiO_2 without immobilized N3 and without catalyst.

While without any additive 48 h of irradiation has been necessary for a complete conversion, small amounts of urea 10^{-6} mol% or thiourea 10^{-4} mol% relating to nitrobenzene lead to quantitative conversion (Table 4, entries 4 - 8). Similar effects were noticed with DMU, TMU and DMSO, but not with more complex derivatives of urea, such as cucurbit[6]uril or cyanuric acid. 4-Substituted nitroarenes are cleanly reduced under the experimental conditions with 10^{-4} mol% thiourea (Table 5), while aldehydes require an electron poor arene, such as in pyridine, for sufficient conversion. This corresponds to previously reported selectivities in related systems.[28]

Table 5. Photoreduction of nitroarenes with N3-modified TiO_2 in the presence of 10^{-4} mol% thiourea.

4-R-C_6H_4-NO_2	**Conversion to 4-R-C_6H_4-NH_2 [%][a]**
R =	
CO_2Et	99
CN	99
Br	62
aldehyde	**Conversion to corresponding alcohol [%]**
C_6H_5-CHO	12
4-CHO-pyridine	85

[a] Reaction monitoring by gas chromatography after 24 h; the given values are the average from three independent reactions.

Acceleration factors, calculated from the ratios of the reaction constants with additive to the reaction constant without additive, are 2.8 for 10^{-4} mol% thiourea, 10^{-4} mol% TMU and 10^{-6} mol% DMSO, which are in the order of metal ion additives like 10^{-4} mol% $AuCl_3$ 2.3 under the same conditions (Table 3). The reaction kinetics of nitrobenzene reductions in identical photocatalytic setups with added 10^{-4} mol% $AuCl_3$, 10^{-4} mol% thiourea or 10^{-6} mol% DMSO were monitored over 24 h (Figure 2) revealing a significant difference: With the gold salt an induction period of slow conversion during 10 - 12 h is observed, while in the presence of thiourea and DMSO the rate of conversion is constant during the irradiation time.[29] The slow initial rate in the case of gold(III) chloride is explained by the slow formation of catalytically active metal clusters (Au^0_n) under the reductive conditions and the buildup of dihydrogen gas pressure.[30] No H_2 gas was detected during the photoreactions in the presence of urea derivatives or DMSO, which indicates another mechanism of nitrobenzene reduction.[31] CV measurements did not show any redox wave for urea, DMU, TMU and DMSO, except thiourea, in the window of -2 to +2 V.

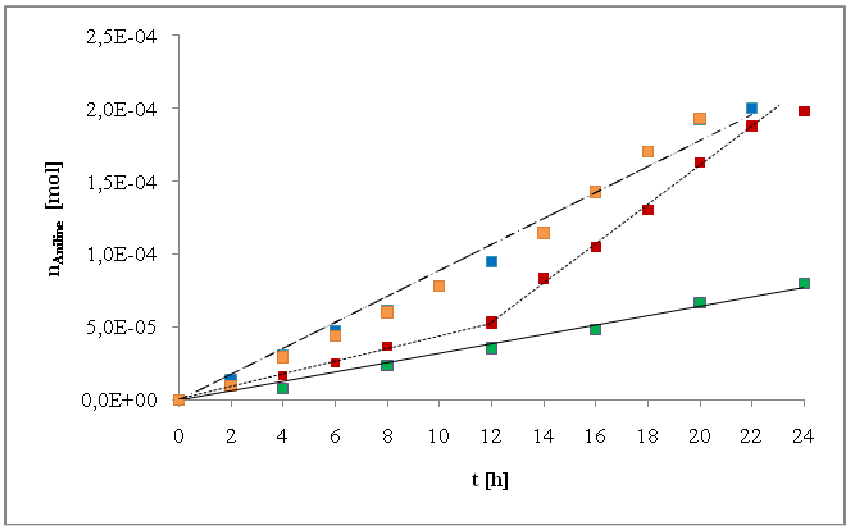

Figure 3. Reaction kinetics of the dye-sensitized TiO_2 photoreduction of nitrobenzene in the presence of 10^{-4} mol% $AuCl_3$ (red, ····), 10^{-4} mol% thiourea (blue,-···-···-), 10^{-6} mol% DMSO (yellow,-·-·) and without catalyst (green, continuous line). $^{a}n_{aniline}$ [mmol] per $n_{nitrobenzene}$ [mmol] calculated from signal integrals in GC chromatogram and an external standard.

CV- and spectrophotometric titrations of nitrobenzene with thiourea in steps of 10 mol% to nitrobenzene showed no significant changes in the redox waves (Figure 4). Furthermore, spectrophotometric and CV-titrations of dye N3 with thiourea revealed no changes in the absorption, fluorescence and redox properties of the ruthenium complex. Thus urea as the role of electron transfer (ET) mediator has been excluded in our photoreductions.[26]

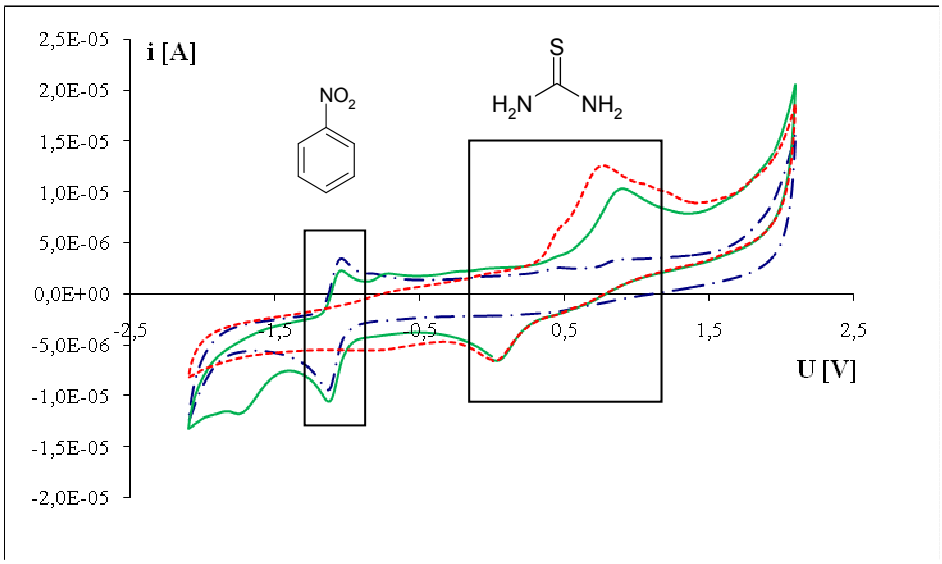

Figure 4. CV-titration spectra of nitrobenzene and thiourea in acetonitrile: (a) thiourea 0.01M (red dotted line), (b) nitrobenzene 0.01 M (blue line -·-·-) and (c) nitrobenzene and thiourea each 0.01 M (green continuous line).

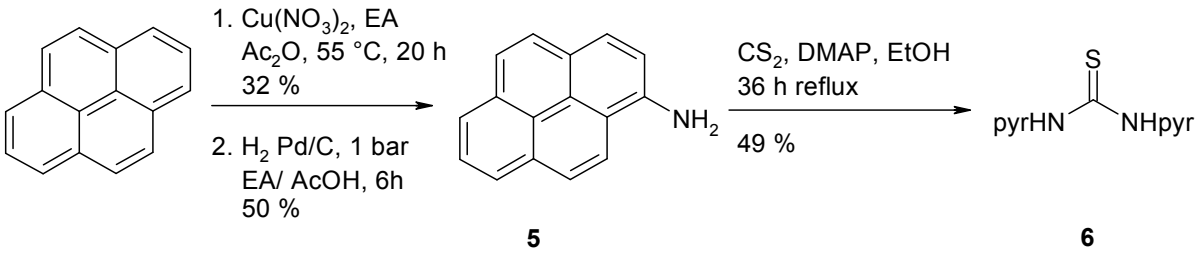

Scheme 3. Synthesis of pyrene (pyr) labeled thiourea.

A surface modification effect of the TiO_2 by urea described by Wen et al.[32] can be also be excluded as the origin of the rate enhancement, as no accumulation of a pyrene labeled thiourea from solution on the semiconductor surface was found using AFM and fluorescence microscopy. Furthermore, we investigated the role of thiourea in a homogeneous photocatalytic system consisting of a dye, TEOA, methylviologen, thiourea and nitrobenzene, which, without nitrobenzene and thiourea but with platinum oxide, has already been investigated for hydrogen evolution from water. $Rubpy_3Cl_2 \cdot 6H_2O$ has been chosen as a dye because of its known redox chemistry and better solubility compared to N3 and methylviologen as the electron transfer substituent for TiO_2 (Table 3). Conversions of 54 % have been obtained without any thiourea and irradiation with 440 nm LEDs.

Table 3. Photoreduction of nitrobenzene with MV^{2+}, TEOA, $Rubpy_3^{2+}$ [a] and thiuorea.

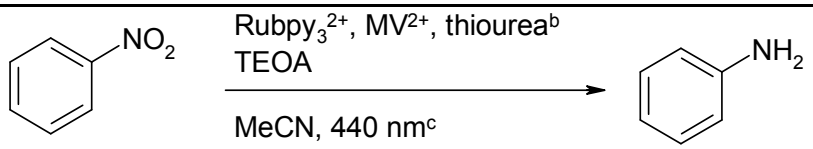

Entry	Amount thiourea [mol%][c]	Conversion [%][d]
1	-	54
2	10^{-3}	98
3	10^{-5}	92

[a] 8 mol% of nitrobenzene. [c] High power LED 3 Watts electric power. [d] Integration of signals in GC chromatograms.

An acceleration of the photocatalytic reduction of nitrobenzene to aniline has been obtained when adding small amounts of thiourea: 98 % aniline for 10^{-3} mol% and 92 % aniline for 10^{-5} mol% thiourea. This effect definitly excludes the role of thiourea as an surface modification agent for TiO_2.

Next, we investigated the effect of added urea derivatives on proton transfer steps, as the electron transfer pathway and the interface seem to be not affected. The use of deuterated

triethanolamine (TEOA-D3) as electron and proton source under identical reaction conditions showed two effects: (1) The amino group of the aniline was fully deuterated, as confirmed by GC-MS and (2) The rate of conversion of nitrobenzene to aniline decreased. The observed kinetic isotopic effects are 2.7 for the non-catalyzed photoreduction, 2.4 for 10^{-4} mol% thiourea, 1.8 for 10^{-4} mol% TMU and 1.9 for 10^{-6} mol% DMSO as additives (Table 4), wich is due to the known lower acidity of deuterated alcohols compared to their ROH.[33] The kinetic isotope effect indicates that the proton transfer is rate determining in the photoreduction reaction.

Table 4. Photoreduction of nitrobenzene with N3-modified TiO_2 and TEOA-H3 or TEOA-D3.

Catalyst [mol%][a]	Reaction rate x10^{-9} [mol/s][b]		Acceleration factor[c]		H/D-ratio[d]
	TEOA-H3	TEOA-D3	TEOA-H3	TEOA-D3	
none	0.99	0.36	-	-	2.7
TU 10^{-4}	2.68	1.12	2.8	3.1	2.4
TMU 10^{-4}	2.76	1.53	2.8	4.2	1.8
DMSO 10^{-6}	2.69	1.42	2.8	3.9	1.9
Au^{3+} 10^{-4}	2.26	1.26	2.3	3.5	1.8

[a] Related to nitrobenzene. [b] Reaction monitored by GC-MS, calculated from integration from three independent reactions; reaction rate from the kinetic plots after 20 h of irradiation. [c] Acceleration rate determined by the ratios of $k[TEOA\text{-}H3]_{additiv}/k[TEOA\text{-}H3]_{no\text{-}catalyst}$ for each system. [d] Kinetic isotopic effect k[TEOA-H3]/k[TEOA-D3] for each catalytic system.

The ET pathway has been investigated previously; the reduction of nitrobenzene proceeds stepwise with intermediates as nitrosobenzene and phenylhydroxylamine.[34] The first electron transfer from the conduction band of TiO_2 to nitrobenzene is slow with a rate of 1.45 x 10^{-8} s^{-1} of pseudo-first-order and a favorable difference in redox potentials $\Delta E = E_{nitrobenzene} - E_{CB\text{-}TiO2}$ = 0.35 V (in water) and $\Delta E = E_{nitrobenzene} - E_{CB\text{-}TiO2}$ = 0.16 V (in acetonitrile) (Table 4). This difference slightly increase in subsequent reduction steps as the reduction of intermediates nitrosobenzene and phenylhydroxylamine are more favorable, which can be seen from the measured redox potentials and calculated values for ΔE and ΔG (Table 5). Solvents affect significantly the redox potential as it has been reported already for TiO_2 and CdS.[35] Nevertheless, from the increase of the thermodynamic driving force ΔG the first electron transfer step from CB_{TiO2} to nitrobenzene seems to be thermodynamically less favourable than the subsequent reductions of the intermediates nitrosobenzenes and phenylhydroxylamines.[37]

Table 5. Redox potentials and ΔG values of nitrobenzene and intermediates in reductions.

Entry	Substance	E_{H2O} [V]	ΔE_{H2O} [V][a]	ΔG_{H2O} [kJ·mol^{-1}][b]	E_{MeCN} [V]	ΔE_{MeCN} [V][a]	ΔG_{MeCN} [kJ·mol^{-1}][b]
1	nitrobenzene	-0.5[34]	0.35	-33.8	-1.09[36]	0.16	-15.4
2	nitrosobenzene	-0.11[37]	0.74	-71.4	-0.949[38]	0.3	-28.9
3	phenylhydroxyl-amine	-0.09[37]	0.76	-73.3	-		
4	CB_{TiO2}	-0.85[34]			-1.25[38]		

[a] Calculated by $\Delta E = E_{substance} - E_{CBTiO2}$. [b] Calculated by $\Delta G = -z \cdot F \cdot \Delta E$, where z = 1 for one electron injection and F = 96484.52 C·mol^{-1}.

However, the proton transfer to the reduction intermediates remains the rate limiting step in these photoreactions and is accelerated by additions of small urea derivatives and DMSO, which results in an overall acceleration of the photoreduction of nitrobenzene to aniline. This acceleration of proton transfer by urea and DMSO has been described for other systems.[39] We therefore suggest a similar effect of the added urea and DMSO in our system leading to an overall acceleration of the photoreduction reaction.

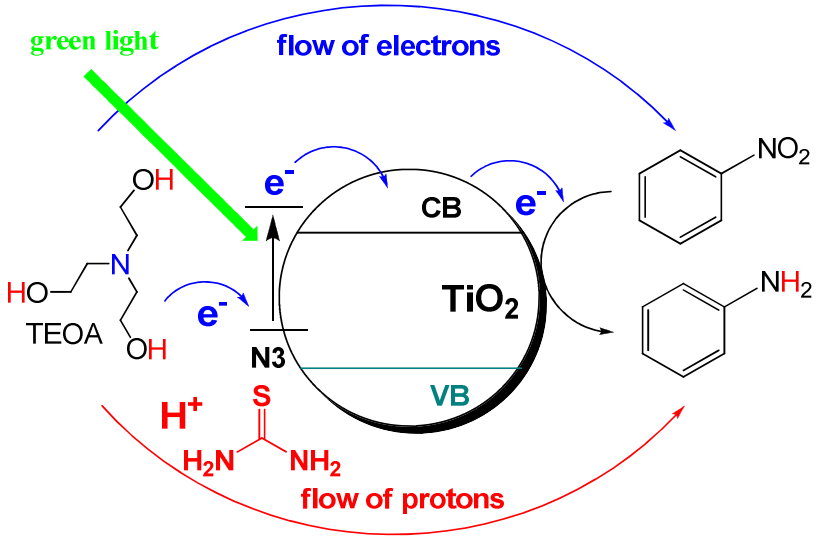

Scheme 3. Proposed mechanism of the green-light-induced reductions of nitrobenzenes via dye-sensitized TiO_2 and nanomolar amounts of urea derivatives.

1.3.2 Conclusion

The combination of ruthenium dye-sensitized TiO_2, as used in the photovoltaic Grätzel cell,[40] with urea derivatives and DMSO as proton transfer agents led to photoreduction catalysts that work with green light irradiation. The catalysts are simple to prepare and apply, and allow the complete, selective and clean conversion of nitrobenzene derivatives to the corresponding anilines. The use of green light irradiation of low energy avoids the formation of unwanted side products and rapid catalyst decomposition. The urea mediated photocatalytic system is well suited for the photocatalytic reduction of nitrobenzene derivatives to their anilines.

1.4 Experimental Part

1.4.1 General Methods and Instruments

1.4.1.1 Spectroscopic and Analytic Methods

NMR-Spectroscopy

For NMR-spectroscopy a Bruker Avance 300 (^{1}H: 300 MHz, ^{13}C: 75 MHz, T = 295 K), was utilized. The chemical shifts are reported in δ [ppm] relative to internal standards (solvent residual peak). The spectra were analysed by first order, the coupling constants *J* are given in Hertz [Hz]. Characterisation of the signals:

s = singlet, d = doublet, t = triplet, dt = double triplet, tt = triple triplet, q = quartet, quint = quintet, m = multiplet.

Integration is determined as the relative number of protons. Error of reported values: chemical shift: 0.01 ppm for ^{1}H-NMR, 0.1 for ^{13}C-NMR, 0.01 ppm for ^{31}P NMR and 0.1 Hz for coupling constants. The solvent used is reported for each spectrum.

Absorption Spectroscopy

Spectra were recorded on a Varian Cary BIO 50 UV/VIS/NIR spectrometer, 1 cm quartz cuvette (Hellma) was used.

Gas Chromatography

(GC I): The measurements were done on a GC 6890 from Agilent Technologies. Injector-temperature (splitinjection: 40:1 split) was 250 °C, detection temperature was at 300 °C (FID). A capillary column Varian Factor Four VF-5MS / 30 m x 0.25mm / 0.2 µm film was used. As carrier gas Helium was utilized with a flow rate of 1 mL/ min. The software Agilent ChemStation Rev.B.04.02. (96) was used for data acquisition and evaluation.

GC measurements were made and investigated via integration of the signals obtained. The GC oven temperature program adjustment was as follows: The initial temperature of 40 °C was kept for 3 minutes. Then the temperature increased constantly at a rate of 15 °C/min for 16 minutes. The final temperature was 280 °C. This temperature was kept for 5 minutes.

TEM Measurements

The sample solution drops were placed on Formvar- and carbon-coated positively glow-discharge treated cupper grid (400 mesh) and subsequently blotted dry with a filter paper. The samples were examined in a LEO912AB electron microscope (Zeiss, Oberkochen/Germany)

operating at 100 kV, equipped with a bottom-mounted CCD-camera capable to record images with 1k x 1k pixels. The documentation was done with the iTEM-software, Ver. 5.0 (Olympus Soft Imaging Solutions GmbH, Muenster/Germany).

1.4.1.2 Solvents and Substrates

Commercial reagents and starting materials were purchased from Aldrich, Fluka, VWR or Acros and used without further purification. Solvents were used as p.a. grade or dried and distilled as described by common procedures.[41]

1.4.2 Photocatalytic Reductions

General Procedure for the Reduction of Nitrobenzene Derivatives and Alkenes

A mixture of the nitro compound or alkene ($2 \cdot 10^{-4}$ mol), TiO_2 with N3 (50 mg, containing $4 \cdot 10^{-6}$ mol N3), stock solution of the transition metal salt or urea derivative, TEOA ($2 \cdot 10^{-3}$ mol) and 2.5 mL MeCN were transferred into a glass vial. The reaction mixture was frozen in liquid nitrogen, evacuated and allowed to warm up to room temperature at 50 mbar. The procedure was repeated and finally the reaction vial was flushed with nitrogen. The sample was irradiated with a high power LED (Luxeon, 3 W, 530 nm) for 24 h. 500 µL of the reaction mixture were diluted with 500 µL $6.7 \cdot 10^{-2}$ M stock solution of toluene in MeCN as standard. 1 µL was injected into the GC/ GC-MS.

General Procedure for the Reduction of Nitrobenzene in large Scales

A mixture of the nitrobenzene ($2 \cdot 10^{-3}$ mol), TiO_2 with N3 (500 mg, containing $4 \cdot 10^{-5}$ mol N3), stock solution of the transition metal salt or urea derivative, TEOA ($2 \cdot 10^{-2}$ mol) and 10 mL MeCN were transferred into a glass vial. The reaction mixture was frozen in liquid nitrogen, evacuated and allowed to warm up to room temperature at 150 mbar. The procedure was repeated and finally the reaction vial was flushed with nitrogen. The sample was irradiated with a high power LED (Luxeon, 3 W, 530 nm) for 36 h. The N3/TiO_2 was filtered off over Celite, the filtrate was evaporated and distilled under high vacuum. Analytical data of all isolated compounds correspond to literature values.

General Procedure for the Kinetic Measurements of the Reduction of Nitrobenzene

A mixture of the nitrobenzene stock solution (500 µL 0.4 M in MeCN), TiO_2 with N3 (50 mg, containing $4 \cdot 10^{-6}$ mol N3), stock solution of the transition metal salt or urea derivative, TEOA ($2 \cdot 10^{-3}$ mol) and 2.5 mL MeCN were transferred into a glass vial. The reaction mixture was frozen in liquid nitrogen, evacuated and allowed to warm up to room temperature at 50 mbar. The procedure was repeated and finally the reaction vial was flushed with nitrogen. The sample was irradiated with a high power LED (Luxeon, 3 W, 530 nm) for 1 h. 30 µL of the reaction mixture were diluted with 60 µL $6.7 \cdot 10^{-2}$ M stock solution of toluene in MeCN as standard. 1 µL was injected into the GC/ GC-MS.

The procedure was repeated to 24 hours, the conversions were calculated from the integrated peaks of the chromatogram.

1.4.3 Deuteration Experiments

Synthesis of Triethanolamine-D3 3

SF 243

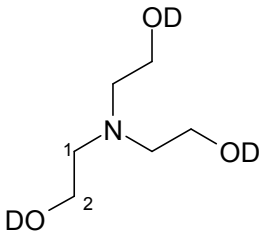

3

TEOA (2 g, $13 \cdot 10^{-3}$ mol) was dissolved in 2.5 ml D_2O, frozen by liquid nitrogen and lyophilized. The procedure was repeated three times and the remaining colorless oil was checked by ^{1}H-NMR-spectroscopy.

^{1}H NMR (300 MHz, CD_3CN, 25 °C, TMS): δ = 2.57 (t, *J* = 7.1 Hz, 6 H, 2-H), 3.50 (t, *J* = 7.1 Hz, 6 H, 1-H).

TEOA-D3 (305 mg, $2 \cdot 10^{-3}$ mol), urea derivative (stock solution), starting material ($2 \cdot 10^{-4}$ mol), immobil. TiO_2 (50 mg) and 2.5 ml acetonitrile were placed in the reaction vial, sealed with a septum and cooled by liquid nitrogen. The mixture was allowed to warm up to room temperature under 50 mbar and flushed with nitrogen. This procedure was repeated one time,

then the cell was irradiated under stirring for 24 h with the high power LED (530 nm, 3 Watts electrical power, 80 lumen).

For analyzing, 500 µl of the reaction mixture were taken out directly by Eppendorf pipette and mixed with 500 µl of a standard (toluene). 1 µl of this solution was injected in the GC/MS. The signals were integrated from the chromatogram.

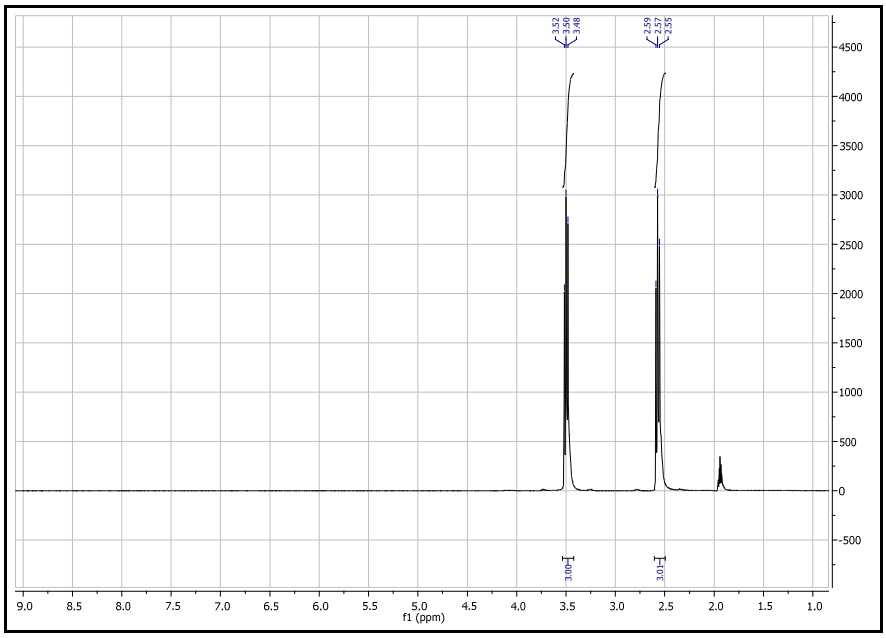

^{1}H-NMR-spectrum of deuterated TEOA (in CD_3CN).

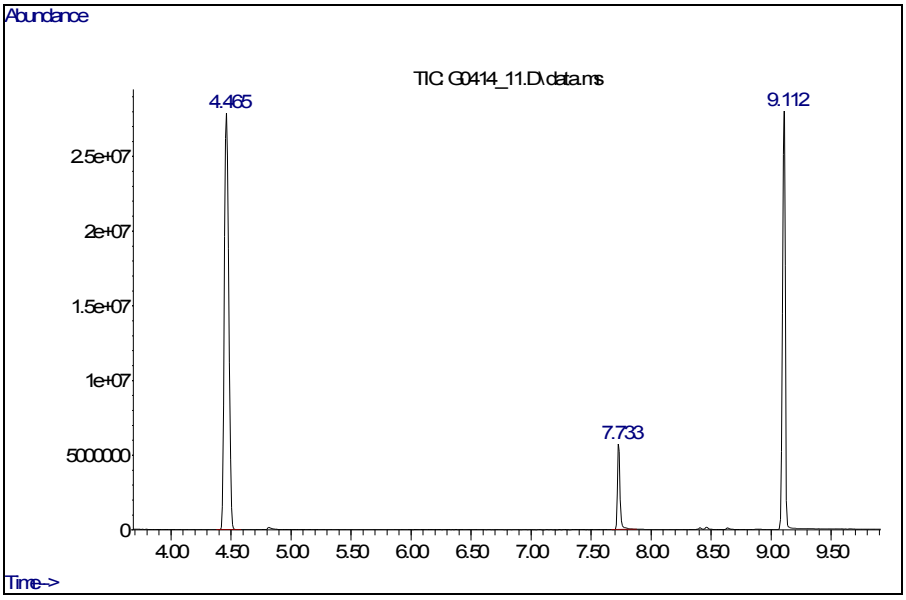

GC-chromatogram of the conversion of nitrobenzene to deuterated aniline via TEOA-D3, dye-sensitized TiO_2 and without catalyst after 14 h of irradiation: toluene t = 4.465 min, deuterated aniline t = 7.733 min and nitrobenzene t = 9.112 min.

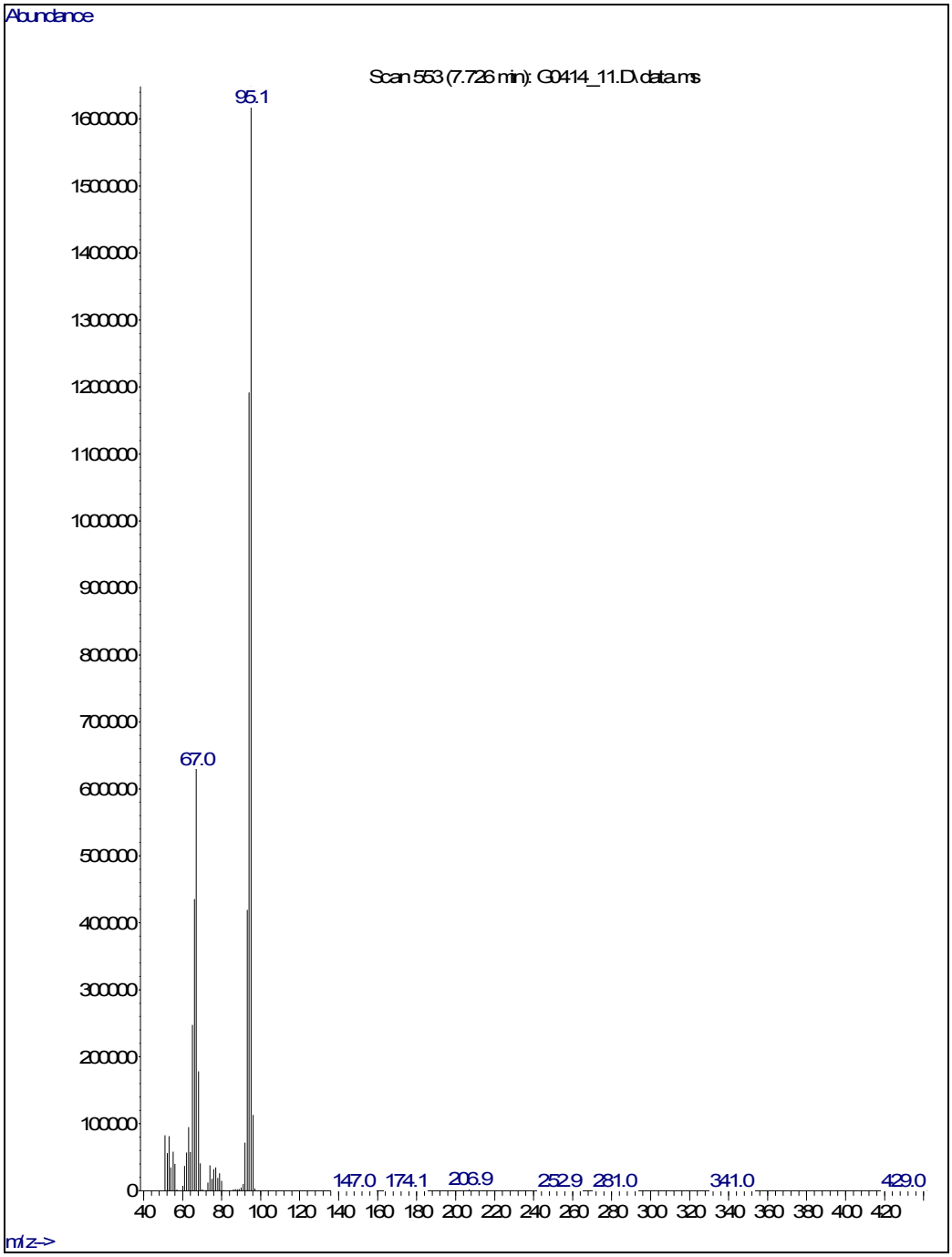

Mass spectrum of peak t = 7.733 min of the GC-chromatogram above.

1.4.4 Photocatalytic Reductions in homogeneous Systems

Stock solution of nitrobenzene (500 µL 0.4 M in MeCN, 0.2 mmol), toluene (500 µL 0.4 M in MeCN, 0.2 mmol) and $[Ru(bipy)_3]Cl_2 \cdot 6H_2O$ (1 mL $1.6 \cdot 10^{-3}$M in MeCN, $1.6 \cdot 10^{-3}$ mmol) were mixed, TEOA (0.25 g, 1.68 mmol) and a solution of $MVCl_2$ (25.6 mg, 0.1 mmol) in aqueous phosphate buffer (pH = 7, 1 mL) were added. Stock solutions of thiourea with 10^{-3} or 10^{-5} mol % in MeCN (related to nitrobenzene) were added to the reaction mixture. The reaction vials

were covered with rubber septa, freeze-pump-thaw was done 2 times, the vial flushed with nitrogen gas and irradiated with blue LEDs (440 nm) for 6 hours. The product mixture was filtered and 1 µL was injected into the gas chromatography (GC).

1.4.4 Synthesis of the dye N3 and Immobilization on TiO_2

1.4.4.1 Synthesis of the Dye

4,4'-Dicarboxylic acid-2,2'-bipyridine 1

SF-10

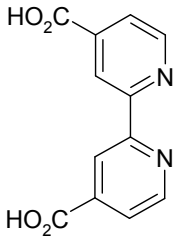

1

4,4'-Dimethyl-2,2'-bipyridyl (2 g, 10.9 mmol) in 50 mL conc. H_2SO_4 was heated to 70 °C. At this temperature $K_2Cr_2O_4$ (9.6 g, 33 mmol) was added slowly and the solution stirred for another hour at this temperature. The hot solution was purred into 300 mL crushed ice and stirred for 1 hour. The green-yellow solid was filtered and washed with 2x 50 mL water. The yellow residue was refluxed in 50 % HNO_3 for 4 hours, cooled to room temperature and purred into 300 mL crushed ice. Crystals were obtained from this water phase over night.
The solid was filtered and dried at high vacuum ($8 \cdot 10^{-2}$ mbar) for 4 h at room temperature. 2.3 g of a colorless solid was obtained (yield: 87 %; lit.[42]: 90 %). Mass analysis and melting point were identical to the reported data: m/z = 244.1; m.p. = 97 °C.

cis-Diaquadithiocyanatobis(2,2'-bipyridyl-4,4'-dicarboxylate)-ruthenium(II) (N3)

SF-11a/11b

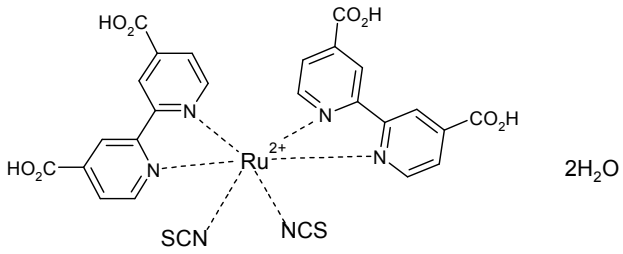

N3

4,4'-Dicarboxylic acid-2,2'-bipyridine **1** (2.3 g, 9.4 mmol) and $RuCl_3 \cdot H_2O$ (1.01 g, 4.5 mmol) were suspended in 25 mL DMF and refluxed overnight. DMF was evaporated, the dark solid dried at high vacuum ($5 \cdot 10^{-2}$ mbar, room temperature) for 2 h. The solid (1.28 g) was used without further purification, dissolved in 160 mL DMF and a solution of NaOH (430 mg, 10.6 mmol) in 100 mL H_2O was added. NaSCN (1.93 g, 23.8 mmol) in 11 mL H_2O was added drop wise under Argon and the solution was allowed to reflux for 6 h. The solvents were evaporated, the crude residue dissolved in 100 mL H_2O and acidified to pH = 2 by $HClO_4$. The dark red solid was filtered, dried at high vacuum and stored in the dark. 1.1 g of a dark solid (**N3**) was obtained (yield: 80 %, lit[43,44]: 80 %). UV- and ESI-MS data of complex **N3** were identical to reported values: m/z = 724.1 ($M + NH_4^+$): UV-VIS (MeCN): α_{max} (nm)/ ε (M^{-1} cm^{-1}) = 546/ 14.000; 401/ 13.800; 316/ 31.000.

1.4.4.2 Synthesis of the Pyrene substituted Thiourea

1-Nitropyrene 4

SF-MK-1

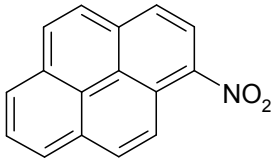

4

To a mixture of pyrene (3 g, 15.0 mmol) and acetic anhydride (4 mL, 42.4 mmol) in ethyl acetate (30 mL) $Cu(NO_3)_2 \cdot 3H_2O$ (5 g, 21 mmol) was added under stirring. Then the system was evacuated - flushed with N_2 three times, stirred and heated at 55 °C for 20 h under nitrogen atmosphere. Yellow precipitate was formed during the reaction. The reaction mixture was cooled to room temperature, the precipitate was filtered off and washed several times with ethyl acetate. The filtrates were collected and extracted with water, saturated $NaHCO_3$ aqueous solution and finally dried over $MgSO_4$. Evaporation under reduced pressure to and purification on silica gel PE/EA = 8:1) gave the pure product (1.17 g, 32 %, Lit.[45]: 93 %).

$C_{18}H_9NO_2$

M = 271,20 g/mol.

R_f = 0.8 (PE/EA 8:1).

^{1}H NMR (300 MHz, DMSO, 25 °C, TMS): δ = 8.19-8.23 (m, 2 H), 8.39-8.43 (m, 2 H), 8.48-8.51 (m, 2 H), 8.78 (m, 3 H).

1-Aminopyrene 5

SF-MK-2

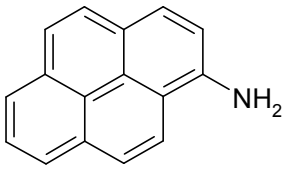

5

In an autoclave a solution of 1-nitropyrene **4** (1g, 5.79 mmol) in ethyl acetate (20 mL) and acetic acid (1.25 mL) was prepared and 10% Pd/C (0.431 g, 0.36 mmol) was added. The system was filled with H_2 (15 bar) and stirred for 6 hours at room temperature. The resulting dark yellow solution was filtered from catalyst, evaporated under reduced pressure to dryness. The solid was crystallized from PE (40-50 mL) to give pure 440 mg product (yield: 50 %, lit.[46]: 80 %).

$C_{18}H_{11}N$

M = 269,2 g/mol.

R_f = 0.9 (PE/EA 8:1).

^{1}H NMR (300 MHz, DMSO, 25 °C, TMS): δ = 4.51 (s, 2 H, N**H**$_2$), 7.42 (d, 1 H), 7.72 (d, 2 H), 7.82-8.12 (m, 7 H).

***N,N'*-bis-(1-pyrenyl)-thiourea 6**

SF-MK-3

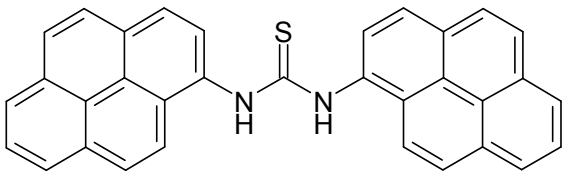

6

A mixture of 1-aminopyrene **5** (0.25 g, 1.15 mmol), CS_2 (0.222 mL, 3.69 mmol) and DMAP (0.12 g, 1 mmol) was dissolved in absolute ethanol and refluxed under stirring in nitrogen atmosphere for 36 hours. The resulting solution was cooled to room temperature and put into refrigerator overnight. The obtained yellowish precipitate was filtered, washed with ethanol and acetone and dried in vacuum to give 130 mg of the pure product (yield: 49 %, lit.[46]: 55 %).

$C_{33}H_{20}N_2S$
M = 476.13 g/mol.

^{1}H NMR (300 MHz, DMSO, 25 °C, TMS): δ = 2.57 (s, 4 H, N**H**$_2$), 8.12-8.19 (m, 1 H), 8.20-8.24 (m, 3 H), 8.31-8.42 (m, 5 H).

ESI-MS: m/z = 477 (MH^+), 953.8 ($2MH^+$).

1.4.5 Dye Immobilization on TiO_2

TiO_2 (4 g, 50 mmol) and dye **N3** (229 mg, $3.2 \cdot 10^{-4}$ mol) were suspended in 25 mL MeCN and stirred for 12 h in the dark under inert atmosphere. The solvent was evaporated, 20 mL toluene was added, evaporated to dryness, the procedure repeated for 3 times and the remaining violet solid dried at high-vacuum ($2 \cdot 10^{-2}$ mbar). The powder was stored in the dark.

1.5 References

[1] A. Pfennig, *Chem. Ing. Technik* **2007,** *79,* 2009-2017.

[2] S. Westenhoff, I. A. Howard, J. M. Hodgkiss, K. R. Kirov, H. A. Bronstein, C. K. Williams, N. C. Greenhorn, R. H. Friend, *J. Am. Chem. Soc.* **2008,** *130,* 13653-13658.

[3] P. Esser, B. Pohlmann, H.-D. Scharf, *Angew. Chem.* **1994,** *106,* 2093-2108.

[4] a) A. L. Linsebigler, G. Lu, J. T. Yates, *Chem. Rev.* **1995,** *95(3),* 735-758. b) M. Barbeni, M. Morello, E. Pramauro, M. Vincenti, E. Borgarello, N. Serpone, Chemosphere **1987,** *Vol 16, No 6,* 1165-1179.

[5] T. Yuranova, R. Mosteo, J. Bandava, D. Laub, J. Kiwi, *J. Mol. Cat. A* **2006,** *244,* 160-167.

[6] a) B. Kayes, M. Filler, *Nature* **2008,** *452,* 400-402. b) M. Hambourger, P. A. Liddell, D. Gust, A. L. Moore, T. A. Moore, *Photochem. Photobiol. Sci.* **2007,** *6,* 431-437.

[7] a) M. W. Kanan, D. G. Nocera, *Science* **2008,** *321,* 1072-1075. b) J. Tang, J. R. Durrant, D. R. Klug, *J. Am. Chem. Soc.*, **2008**, *130 (42),* 13885-13891 c) R. Brimblecombe, G. Swiegers, G. C. Dismukes, L. Spiccia, *Angew. Chem.* **2008,** *120,* 7445-7448.

[8] a) S. Rau, D. Walthera, J. G. Vosb**,** *Dalton Trans.* **2007,** 915-919. b) M. A. Ischay, M. E. Anzovino, J. Du, T. P. Yoon, *J. Am. Chem. Soc.* **2008,** *130(39),* 12886-12887. c) H. Schmaderer, P. Hilgers, R. Lechner, B. König, *Adv. Synth. Cat.* **2009,** *351,* 163 - 174. d) G. Imperato, B. König, *ChemSusChem* **2008,** *1*, 993-996. e) J. Svoboda, H. Schmaderer, B. König, *Chem. Eur. J.* **2008,** *14,* 1854-1865. f) R. Cibulka, R. Vasold, B. König, *Chem. Eur. J.* **2004,** *10,* 6223-6231. g) J. Du, T. P. Yoon, *J. Am. Chem. Soc*. **2009**, doi 10.1021/ja903732v.

[9] S. Rau, B. Schäfer, D. Gleich, E. Anders, M. Rudolph, M. Friedrich, H. Görls, W. Henry, J. G. Vos, *Angew. Chem.* **2006,** *118,* 6361-6364.

[10] A. Nicewicz, D. W. C. MacMillan, *Science* **2008,** *322,* 77-80.

[11] a) A. Bauer, F. Westkämpfer, S. Grimme, T. Bach, *Nature* **2005,** *436,* 1139-1140. b) J. Svoboda, B. König, *Chem. Rev.* **2006**, *106*, 5413-5430.

[12] M. Fagnoni, D. Dond, D. Ravelli, A. Albini, *Chem. Rev*. **2007**, *107*, 2725-2756.

[13] Recent review: J.-H. Yum, P. Chen, M. Graetzel, M. K. Nazeeruddin, *ChemSusChem* **2008**, *1*, 699-707.

[14] M. Zhang, C. Chen, W. Ma, J. Zhao, *Angew. Chem.* **2008,** *120,* 9876 -9879.

[15] H.C. Pehlivanugullari, E. Sumer, H. Kisch, *Res. Chem. Intermed.* **2007,** *33,* 297-309.

[16] a) H. Takeda, K. Koike, H. Inoue, O. Ishitani, *J. Am. Chem. Soc.* **2008**, *130,* 2023-2031. b) W. R. McNamara, R. C. Snoeberger, G. Li, J. M. Schleicher, C. W. Cady, M. Poyatos, C. A. Schmuttenmaer, R. H. Crabtree, G. W. Brudvig, V. S. Batista, *J. Am. Chem. Soc.* **2008**, *130*, 14329-14338. c) P. Du, J. Schneider, F. Li, W. Zhao, U. Patel, F. N. Castellano, R. Eisenberg, *J. Am. Chem. Soc.* **2008**, *130*, 5056-5058.

[17] a) P. Du, J. Schneider, F. Li, W. Zhao, U. Patel, F. N. Castellano, R. Eisenberg, *J. Am. Chem. Soc.* **2008**, *130*, 5056-5058. b) O. Ozcan, F. Yukruk, E.U. Akkaya, D. Uner, *Top. Catal.* **2007,** *44(4),* 523-528.

[18] G. Li, N.M. Dimitrijevic, L. Chen, J.M. Nichols, T. Rajh, K.A. Gray, *J. Am. Chem. Soc.* **2008**, *130*, 5402-5403.

[19] a) H. Tada, A. Takao, T. Akita, *ChemPhysChem* **2006,** *7,* 1687-1691. b) H. Tada, T. Ishida, A. Takao, S. Ito, *Langmuir* **2004,** *20,* 7898-7900, c) Y. Matsushita, S. Kumada, K. Wakabayashi, K. Sakeda, T. Ichimura, *Chem. Lett.* **2006,** *35,* 410-411.

[20] P. Swoboda, R. Saf, K. Hummel, *Macromolecules* **1995,** *28,* 4255-4259.

[21] H. Tada, T. Ishida, A. Takao, S. Ito, *Langmuir* **2004,** *20,* 7898-7900.

[22] S. Chen, K. Kimura, *J. Phys. Chem. B* **2001,** *105,* 5397-5403.

[23] E. Kolwaska, H. Remita, C. Colbeau-Justin, J. Hupka, J. Belloni, *J. Phys. Chem. C* **2008,** *112(4),* 1124-1131.

[24] J.I.L. Chen, E. Loso, N. Ebrahim, G.A. Ozin, *J. Am. Chem. Soc.* **2008**, *130*, 5420-5421.

[25] B.H. Kim, Y. Jin, Y.M. Jun, R. Han, W. Baik, B.M. Lee, *Tetrahedron Lett.* **2000,** *41,* 2137-2140.

[26] N.J.A. artin, L. Ozores, B. List, J. *Am. Chem. Soc.* **2007,** *129,* 8976-8977.

[27] X. Yu, W. Wang, *Chem. Asian J.* **2008,** *3,* 516-532.

[28] S. Füldner, R. Mild, H.I. Siegmund, J.A. Schroeder, M. Gruber, B. König, *Green Chem.* **2010,** *12,* 400-406.

[29] Without any additive the conversion was completed only after 48 h (data not shown).

[30] Hydrogen gas was detected by gas chromatography in photoreductions using platinum metal salts.

[31] J. Svoboda, H. Schmaderer, B. König, *Chem. Eur. J.* **2008,** *14(6),* 1854-1865.

[32] J. Wei, L. Zhao, S. Peng, J. Shi, Z. Liu, W. Wen, J Sol-Gel Sci. Technol. **2008**, *47*, 311-315.

[33] A. Yacovan, S. Hoz, *J. Am. Chem. Soc.* **1996,** *118,* 261-262.

[34] (a) S.O. Flores, O. Rios-Bernij, M.A. Valenzuela, I. Córdova, R. Gómez, R. Gutiérrez, *Topics in Catalysis* **2007**, *44,* 507-511. (b) J.L. Ferry, W. Glaze, *Langmuir* **1998,** *14,* 3551-3555.

[35] (a) M.A. Fox, *Top. Curr. Chem.* **1987,** *142,* 71-99. (b) M.J. Natan, J.W. Thackeray, M.S. Wrighton, *J. Phys. Chem.* **1986,** *90,* 4089-1430.

[36] L. Holleck, R. Schindler, O. Löhr, *Naturwissenschaften* **1959,** *46,* 625-626.

[37] J.W. Smith, J.G. Waller, *Trans. Faraday Soc.* **1950,** *46,* 290-295.

[38] V. Brezová, P. Tarábek, D. Dvoranová, A. Staško, S. Biskupič, *J. Photochem. Photobiol A: Chemistry,* **2003,** *155,* 179-198.

[39] (a) N. Kuramoto, S. Nishikawa, *J. Phys. Chem.* **1995,** *99,* 14372-14376. (b) M.T. Htun, A. Suwaiyan, A. Baig, U.K.A. Klein, *J. Phys. Chem. A.* **1998,** *102,* 8230-8235.

[40] M.K. Nazeeruddin, A. Kay, I. Rodicio, R. Humphry-Baker, E. Müller, P. Liska, N. Vlachopoulos, M. Grätzel, *J. Am. Chem. Soc.* **1993,** *115,* 6382-6390.

[41] K. Schwetlick, *Organikum* **2001,** Wiley-VCH.

[42] H. Kim, Y. Jin, Y.M. Jun, R. Han, W. Baik, B. M. Lee, *Tet. Lett.* **2000,** *41,* 2137-2140.

[43] P. G. Hoertz, A. Staniszewski, A. Marton, G. T. Higgins, C. D. Incarvito, A. L. Rheingold, G.J. Meyer, *J. Am. Chem. Soc.* **2006,** *128,* 8234-8245.

[44] M. K. Nazeeruddin, A. Kay, I. Rodicio, R. Humphry-Baker, E. Müller, P. Lisa, N. Vlachopoulos, M. Grätzel et al., *J. Am. Chem. Soc.* **1993,** *115,* 6382-6390.

[45] P. Babu, N.M. Sangeetha, P. Vijaykumar, U. Maitra, K. Rissanen, A.R. Raju, *Chem. Eur. J.* **2003,** *9,* 1922-1932.

[46] M. Bollini, J.J. Casal, D.E. Alvarez, L. Boiani, M. Gonzalez, H. Cerecetto, A.M. Bruno, *Bio. Med. Chem.* **2009,** *17,* 1437-1444.

2 Selective Photocatalytic Reductions of Nitrobenzene Derivatives using $PbBiO_2X$ and Blue Light

2.1 Introduction

Sunlight is the only sustainable energy resource on earth and photovoltaic systems for the conversion of solar energy into electrical power have evolved into a wide range of applications.[1] Photocatalysts, converting visible light energy into chemical energy, are known, but they are less developed. Recent examples of homogeneous photocatalysts include the hydrogenation of alkynes,[2] the asymmetric alkylation of aldehydes[3] and the dehalogenation of α-alkylated esters.[4] Heterogeneous photocatalysts are typically semiconductors based on modified or unmodified TiO_2 or CdS. Unmodified TiO_2 has been investigated for the reduction of nitrobenzenes to their anilines under UV-light[5] irradiation, whereas modified and dye-sensitized TiO_2 reduces these molecules or oxidizes alcohols with blue or green light.[6] CdS quantum dots have been found to be suitable photocatalysts for the reduction of azides to anilines,[7] but the systems have disadvantages: UV light is only a small part of the solar spectrum, which diminishes the efficiency of unmodified TiO_2 in sunlight. CdS and modified TiO_2 absorbing in the visible range require special preparation. Oxide halides, such as $Pb\mathit{Pn}O_2\mathit{X}$ (*Pn* = Bi, Sb; *X* = Br, Cl) have been structurally characterized and applied for the oxidative photodegradation of organic dyes, e.g. methylene blue and methyl orange.[8] These materials are potential heterogeneous photocatalysts for organic chemical synthesis using visible light and may nicely complement the green-light-induced reductions of nitrobenzene derivatives with dye-sensitized TiO_2.[6]

Here, we report a method for selective reductions of nitro arenes with blue light using $PbBiO_2X$ particles. The simple, but effective heterogeneous photocatalysts are prepared by simple mixing and anneling of PbO, Bi_2O_3 and BiX_3 not requiring any special procedures.[8] Samples were irradiated with High Power LEDs emitting at 440 nm / ± 10 nm. The observed photoconversions of organic substrates are very clean, as verified by gas chromatographic monitoring and in many cases quantitative.

2.2 Results and Discussions

Heterogeneous photocatalysts of the composition $PbPnO_2X$ with *Pn* = Bi, Sb and *X* = Br, Cl, I were synthesized from PbO, Pn_2O_3 and PnX_3 in evacuated silica ampoules by annealing the 3 : 1 : 1 mixtures at 500 - 650 °C for several days[8] and used for the quantitative photoreduction of nitrobenzenes to anilines using blue LED light irradiation or sun light. All $PbPnO_2X$ photocatalysts absorb in the blue range of the visible spectrum (Figure 1).

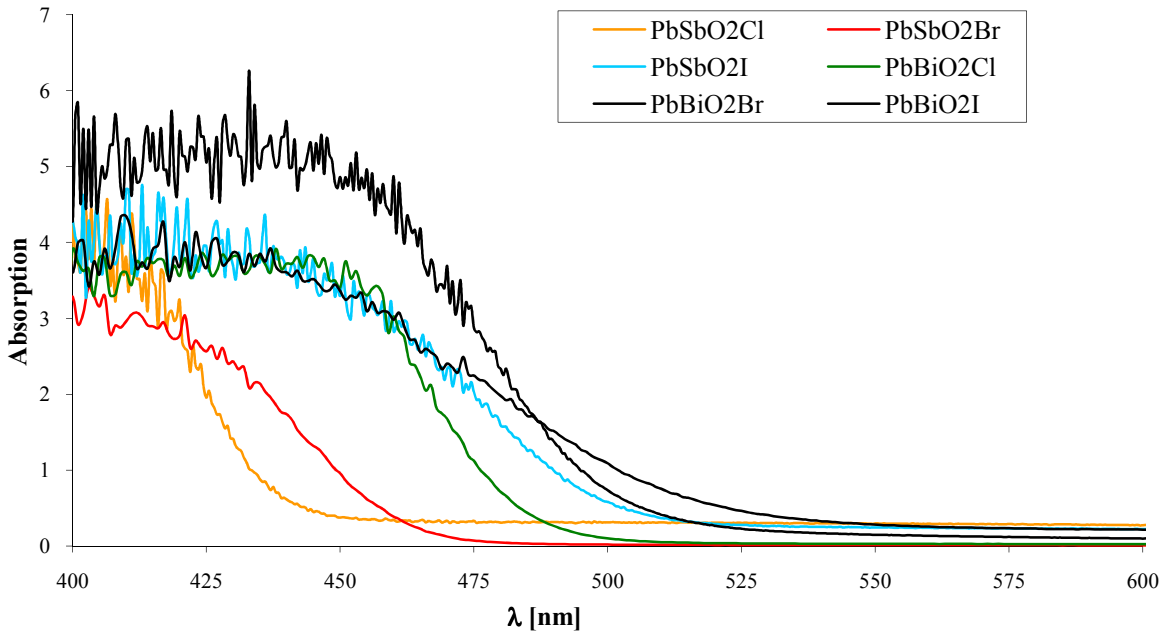

Figure 1. Absorption spectra of $PbPnO_2X$ (*Pn* = Bi, Sb; *X* = Br, Cl, I).

The reduction of nitrobenzene derivatives was chosen to monitor the photocatalysts efficiency, because of the formal sequential transfer of six equivalents of hydrogen.[9] The selective photoreduction of nitrobenzenes is possible using TiO_2 and UV irradiation[10] or dye-sensitized TiO_2 and green light irradiation.[6] All oxide halides have been investigated towards their photocatalytic reductions of nitrobenzenes, but irradiation of samples containing $PbSbO_2X$ (*X* = Br, Cl, I) as catalyst did not lead to any conversion (Table 1, entries 1 - 3). The exchange of Sb^{3+} by Bi^{3+} in the composition of the photocatalyst lead to an almost quantitative conversion of nitrobenzene to aniline within 20 hours of blue light irradiation if *X* was bromide or chloride. In case of *X* = iodide no conversion is observed (Table 1).

Table 1. Photocatalytic reduction of nitrobenzene to aniline via $PbPnO_2X$.

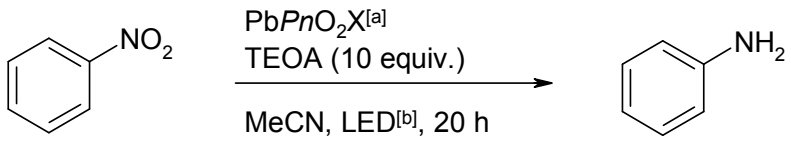

2 x 10^{-4} mol

Entry	$PbPnO_2X$	LED wave-length [nm][b]	Nitrobenzene Conversion [%][c]
1	$PbSbO_2Br$	440	≤ 4
2	$PbSbO_2Cl$	440	≤ 4
3	$PbSbO_2I$	440	≤ 4
4	$PbBiO_2Br$	440	> 99
5	$PbBiO_2Cl$	440	> 99
6	$PbBiO_2I$	440	≤ 1
7	$PbBiO_2I$	530	≤ 1

[a] 50 mg Oxide halide. [b] LED with 3 Watt electrical power, 80 lumen.

[c] Integration of signals in GC-chromatogram.

Previous reports discussed mainly electronic reasons for the different catalytic activities of layered $PbPnO_2X$ type materials (*Pn* = Sb, Bi, *X* = Cl, Br, I).[8,11] However, also crystal-chemical arguments should be taken into consideration to explain the photocatalytic properties of the compounds. A possible reason for the different catalytic activity of the oxides may be derived both from their crystal structures, their optical and their redox properties. All solid materials under discussion crystallize in a layered structure. They exhibit covalent metal oxygen layers $^2_\infty[PbBiO_2^+]$ separated by halide layers which are stacked along [001].[8] One can assume that the crystal surface consists of metal oxygen layers, i.e., the metal atoms are expected to form the (001) surfaces. In case of the bismuth compounds the metal position is statistically occupied by lead and bismuth in the ratio 1 : 1, whereas in the synthetic antimony compounds $PbSbO_2Br$ and $PbSbO_2I$ the antimony atoms are slightly displaced parallel [001] towards the oxygen atoms. By contrast, $PbSbO_2Cl$ has an ordered structure. However, therein the antimony atoms are also displaced towards the oxygen atoms. So the antimony atoms do not reach the outer crystal surface and thus are not accessible for catalytic processes (Figure 2). Photocatalytic measurements with PbO which has a similar layered structure as the polycationic $^2_\infty[PbBiO_2^+]$ sheets in the title compound did not show

any catalytic activity at all, although the absorption spectra are quite similar. So an activity due to Pb^{2+} can be ruled out.

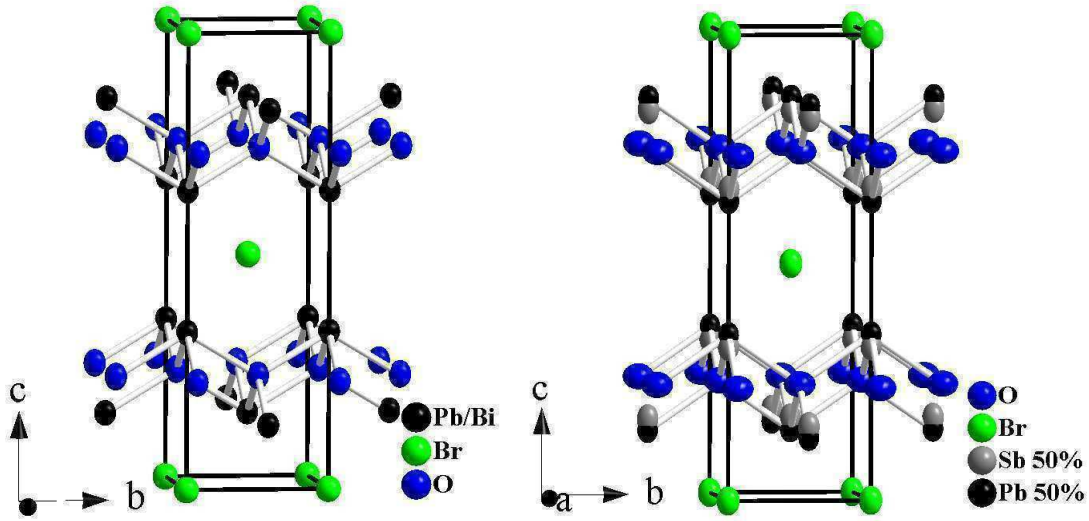

Figure 2. Crystal structures of $PbSbO_2Br$ (right) and $PbBiO_2Br$ (left). Ellipsoid correspond to a probability of 70 %. The position of the metal is occupied statistically by 50 % Bi and 50 % Pb in case of $PbBiO_2X$. In case of $PbSbO_2X$ the positions of Pb and Sb can be resolved.

As the surface is only built by Pb^{2+} (in the antimony containing materials) or both by Pb^{2+} and Bi^{3+} (in bismuth containing materials) it is likely that Bi^{3+} is responsible for the photocatalytic properties in this system. Surprisingly, only $PbBiO_2X$ with X = Cl, Br catalyzed the photoreduction of nitrobenzene to aniline while no conversion occurred for $PbBiO_2I$ when irradiated under comparable conditions. Furthermore, the latter materials absorb a significant part of the visible spectrum, see Figure 1. The experimentally determined optical band gaps are 2.55 eV ($PbBiO_2Cl$), 2.47 eV ($PbBiO_2Br$) and 2.39 eV ($PbBiO_2I$).[11] It seems that the gaps of all these semiconductors are in the right range to catalyze the observed reaction. Therefore, changes in the structural nature of the materials may be decisive: Increasing iodine content in $PbBiO_2X$ leads to a change of the preferred crystal grow directions. Thus, $PbBiO_2Cl$ and $PbBiO_2Br$ form layered crystal along (001), whereas $PbBiO_2I$ crystallizes as rods with [001] as the rod axis. The changes of the bonding interactions between the halide and metal atoms indicate this clearly. In the case of rod like crystals the surface of the material is significantly different: The surface changes from mainly (001) for chloride and bromide to mainly (110) and (010) for iodide, which may alter the catalytic activity. The stronger bonds of iodine to Pb or Bi, well known for binary metal halides, change crystal growth and may inactivate the surface.

Moreover, redox quenching by iodine may intercept the catalysis, too. Therefore, the redox potentials of the oxide halides were measured, revealing multi redox processes which did not allow deriving exact values. However, iodide inactivation has been investigated with semiconductors $PbBiO_2Br_nI_m$ and $PbBiO_2Cl_nI_m$ with varying ratios of their halogen content and analyses of their photocatalytic activities in nitrobenzene reduction. With an increasing amount of iodine in $PbBiO_2Br_nI_m$ and $PbBiO_2Cl_nI_m$ the photocatalytic activity decreased dramatically (Figure 3). Similar effects have been reported for the photodegradation of RhodamineB with BiOX (*X* = Cl, Br and I).[12] These materials crystallize in the same tetragonal structure, their optical band gaps are in the right region for visible light photocatalysis, but only BiOBr and BiOCl showed activities towards oxidative photo-degradation of RhodamineB.

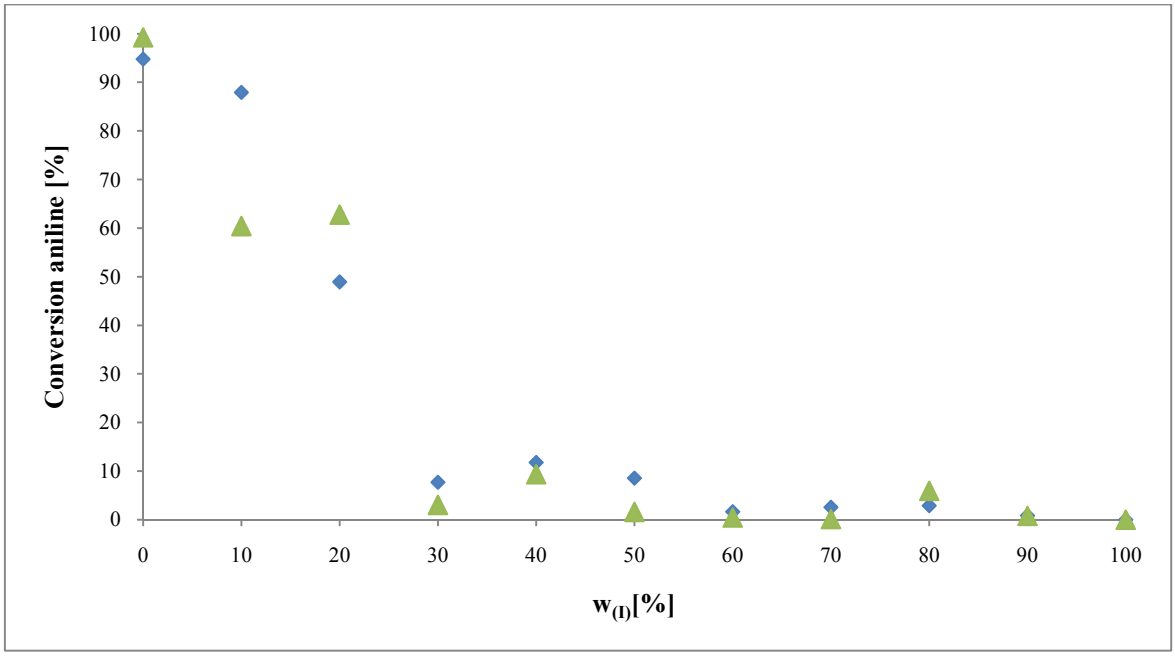

Figure 3. Photoconversion of nitrobenzene after 20 h depending on the iodine content for $PbBiO_2Br_nI_m$ (green) and $PbBiO_2Cl_nI_m$ (blue).

The semiconductors have been investigated in our photoreductions of nitrobenzene to aniline, too, but only in the case of BiOBr and BiOCl full conversions were observed under identical experimental conditions. Irradiation of BiOI did not induce any photocatalytic activity for nitrobenzene reduction. Such electronic quenching in semiconductors photocatalysis has already been reported for UV photodegradation of acid orange[13] and curcumin[14] with TiO_2 in the presence of iodide. Furthermore, the UV-light-induced reduction of nitrobenzene to aniline has been inhibited when adding small amounts of iodide to TiO_2 and TEOA. Hence, the same argument should be valid for the investigated $PbBiO_2X$ semiconductors, as they

show similar redox potentials, band gaps and crystal structures. Therefore, the observed dependence of the $PbBiO_2X$ photoactivity has been related on the iodine content to electronic quenching and changes in their surface properties.

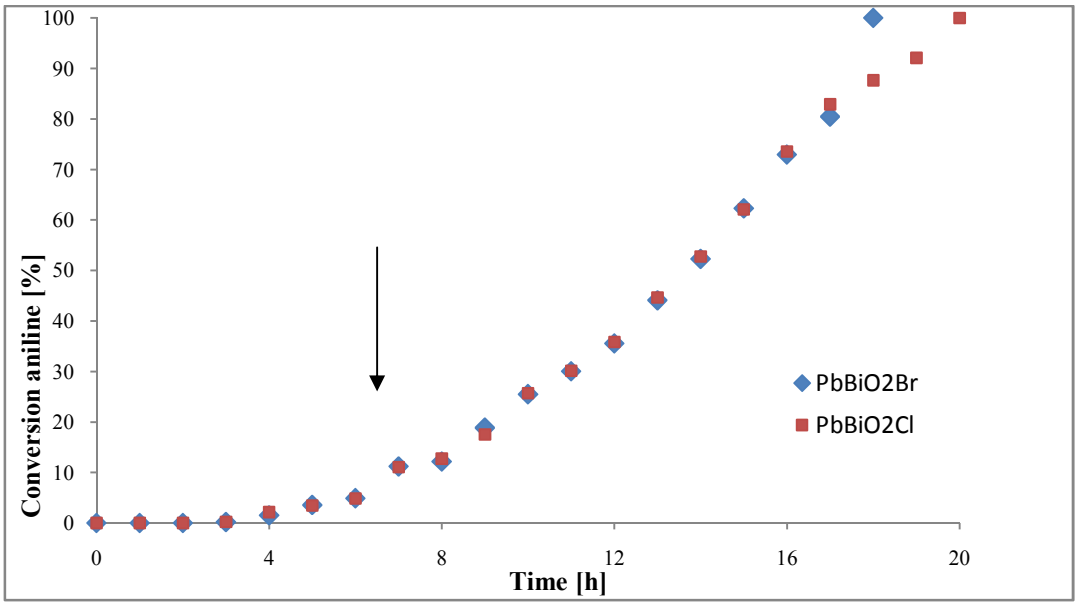

Figure 4. Kinetics of the reduction of nitrobenzene to aniline via $PbBiO_2X$ (X = Br, Cl).

The kinetic analysis of the photo reduction of nitrobenzene to aniline with $PbBiO_2Br$ and $PbBiO_2Cl$ showed an increase in the rate of nitrobenzene to aniline conversion after approx. 6 hours of irradiation with blue light (Figure 4). This induction period indicates catalyst activation or gas evolution as reported in the photoreductions of nitrobenzenes to their anilines via dye-sensitized TiO_2 and metal salts.[6] Head space gas chromatographic analysis revealed the presence of dihydrogen gas after 14 h of irradiation, which explains the selectivity for the exclusive reduction of nitrobenzenes to their corresponding anilines (Table 2).

Table 2. Photoreduction of nitrobenzene derivatives via $PbBiO_2Br$.[a]

Entry	Starting Material[b]	Product [%][c]	
1	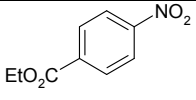	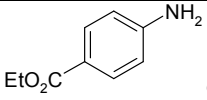 95	
2	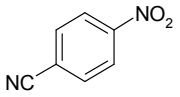	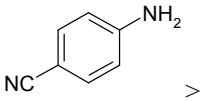 > 99	
3	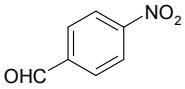	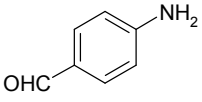 > 99	
4	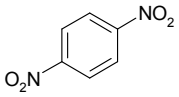	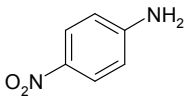 35	
5	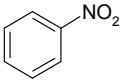	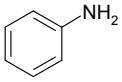 > 99	
6	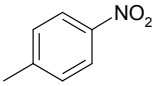	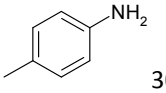 30	
7	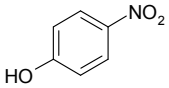	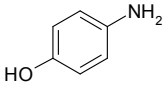 < 1	
8	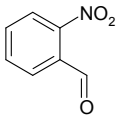	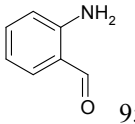 95	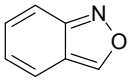 0
9	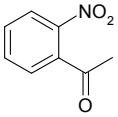	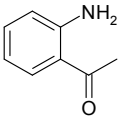 81	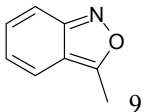 9
10	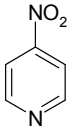	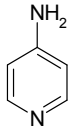 90	
11	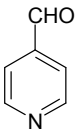	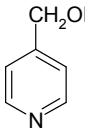 54	
12	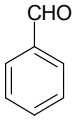	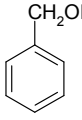 0	

[a] 50 mg and irradiation with 440 nm LED with 3 Watt electrical power, 80 lumen. [b] $2 \cdot 10^{-4}$ mmol.

[c] Integration of signals in GC-/ GC-MS-chromatogram.

Stability of $PbBiO_2Br$ has been investigated by XRD analysis of the semiconductor before and after the photo reaction. After irradiation of 20 h the semiconductor became grey, but

only in the presence of TEOA. The grey color slightly disappeared, when the sample was treated in an ultrasonic bath. X-ray powder diffraction spectra clearly showed no changes in the molecular structure under the experimental conditions (Figure 5).

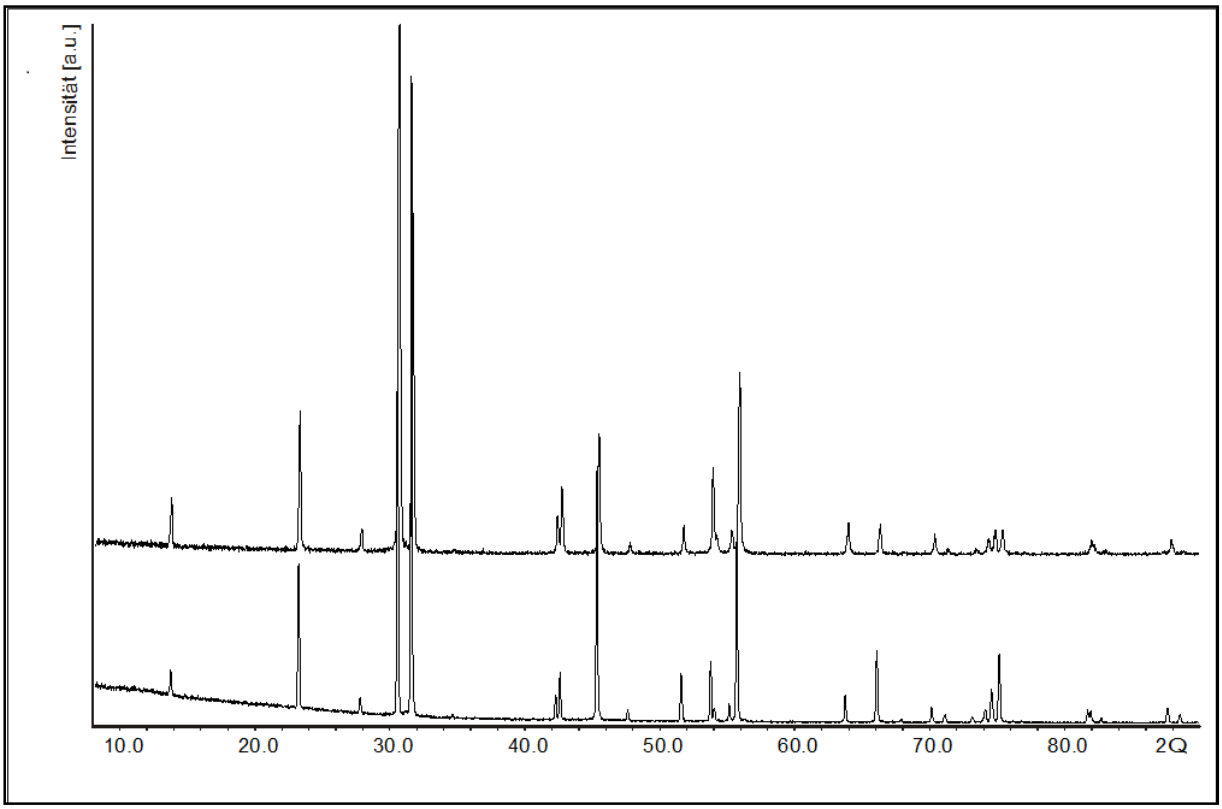

Figure 5. X-ray powder diffraction spectra of $PbBiO_2Br$ before (upper) and after catalysis (lower).

Similar observations have been described in the photocatalytic oxidation of isopropyl alcohol to CO_2 with BiOCl.[12] Therefore, we suggest surface passivation processes on $PbBiO_2Br$ during the photo catalysis.[15]

The maximum number of catalyst reuse was determined: After every catalytic cycle the grey catalyst was filtered, sonicated in an ultrasonic bath and used again for photoreduction of nitrobenzene to aniline. Within five catalytic cycles the photocatalytic activity did not decrease; after eight reuses the conversion under identical experimental conditions decreased to give 50 % conversion. Treatment in the ultrasonic bath is essential to retain the photocatalyst, which otherwise decreased dramatically within 5 cycles (Figure 6).

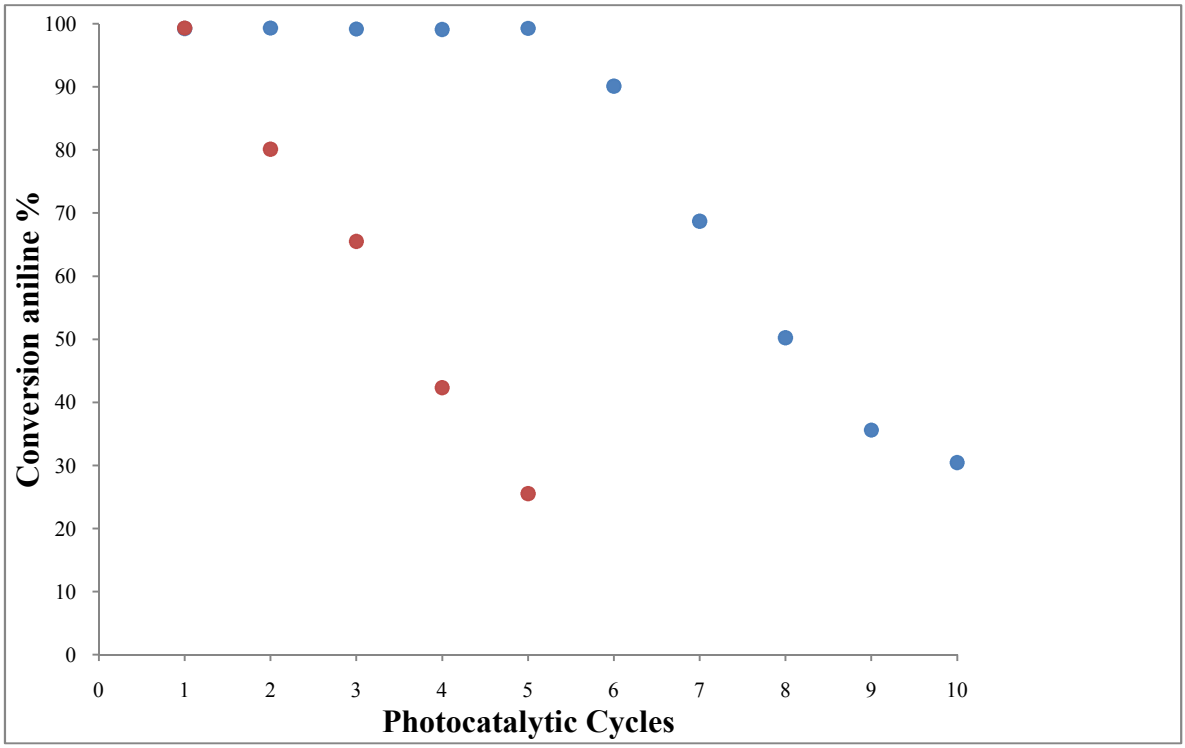

Figure 6. Photocatalyst recycling experiments of $PbBiO_2Br$ (a) with sonication of the catalyst before reuse (blue) (b) reuse without sonication (red).

2.3 Conclusion

Semiconductors of the composition $PbBiO_2X$ (X = Cl, Br) selectively photoreduce nitrobenzenes to anilines in the presence of triethanolamine if irradiated with blue light of low intensity. The photocatalysts are simple to prepare by established solid state chemistry techniques and allow complete and clean conversion of the substrates. Structural studies explain the differences in catalytic activity for related Bi^{3+} and Sb^{3+} compounds. The missing photocatalytic activity of the iodine containing material may be due to redox quenching and surface effects, as indicated by the decrease of photocatalytic activity in $PbBiO_2Br_nI_m$ and $PbBiO_2Cl_nI_m$ with increasing iodine content and an inhibited nitrobenzene photoreduction with TiO_2 in the presence of iodide. The detection of dihydrogen finally explains the exclusive selectivity for nitrobenzene reductions. Recycling experiments revealed a high stability of the photocatalyst over several reuses, but sonication to remove passivations is essential.

The investigations provide a more detailed mechanistic description of this class of heterogeneous semiconductor photocatalysts, which will facilitate the design and prediction of properties of next generations of photocatalysts of this type.

2.4 Experimental Part

2.4.1 General Methods and Instruments

2.4.1.1 Spectroscopic and Analytic Methods

NMR-Spectroscopy

For NMR-spectroscopy a Bruker Avance 300 (^{1}H: 300 MHz, ^{13}C: 75 MHz, T = 295 K), was utilized. The chemical shifts are reported in δ [ppm] relative to internal standards (solvent residual peak). The spectra were analysed by first order, the coupling constants *J* are given in Hertz [Hz]. Characterisation of the signals:

s = singlet, d = doublet, t = triplet, dt = double triplet, tt = triple triplet, q = quartet, quint = quintet, m = multiplet.

Integration is determined as the relative number of protons. Error of reported values: chemical shift: 0.01 ppm for ^{1}H-NMR, 0.1 for ^{13}C-NMR and 0.1 Hz for coupling constants. The solvent used is reported for each spectrum.

Absorption Spectroscopy

Spectra were recorded on a Varian Cary BIO 50 UV/VIS/NIR spectrometer, 1 cm quartz cuvette (Hellma) was used.

Gas Chromatography

(GC I): The measurements were done on a GC 6890 from Agilent Technologies. Injector-temperature (splitinjection: 40:1 split) was 250 °C, detection temperature was at 300 °C (FID). A capillary column Varian Factor Four VF-5MS / 30 m x 0.25mm / 0.2 µm film was used. As carrier gas Helium was utilized with a flow rate of 1 mL/ min. The software Agilent ChemStation Rev.B.04.02. (96) was used for data acquisition and evaluation.

GC measurements were made and investigated via integration of the signals obtained. The GC oven temperature program adjustment was as follows: The initial temperature of 40 °C was kept for 3 minutes. Then the temperature increased constantly at a rate of 15 °C/min for 16 minutes. The final temperature was 280 °C. This temperature was kept for 5 minutes.

2.4.1.2 Solvents and Substrates

Commercial reagents and starting materials were purchased from Aldrich, Fluka, VWR or Acros and used without further purification. Solvents were used as p.a. grade or dried and distilled as described in common procedures.[16]

2.4.2 Syntheses of $PbPnO_2X$

$PbPnO_2X$ ($Pn = Bi^{3+}$, Sb^{3+} and $X = Cl^-$, Br^- and I^-) have been synthesized as described before.[8] X-ray powder diffraction data was collected on a STOE Stadi P ($CuK_{\alpha 1}$, germanium monochromator). Cell constants were determined from powder patterns by least square refinement using the program package $WinX^{POW}$.[17]

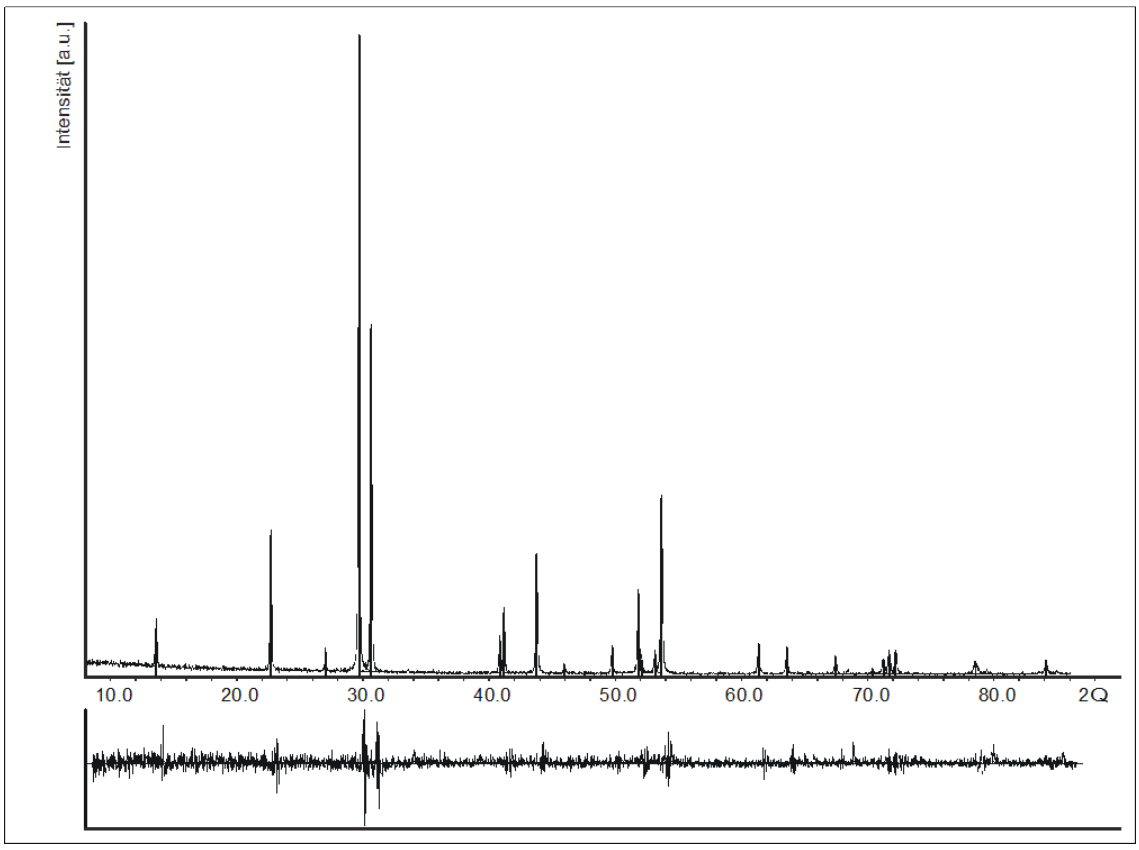

Example of a X-Ray powder diffractogram of $PbBiO_2Br$.

2.4.3 Photocatalytic Reductions

General procedure for the reduction of nitrobenzene derivatives

Triethanolamine (TEOA, 300 mg, $2 \cdot 10^{-3}$ mol), the nitrobenzene derivative ($2 \cdot 10^{-4}$ mol), $PbPnO_2X$ (50 mg) and 2.5 mL of acetonitrile were placed in the reaction vial, sealed with a septum and cooled by liquid nitrogen. The mixture was allowed to warm up to room temperature under 50 mbar and flushed with nitrogen. This procedure was repeated one time, afterwards the cell was irradiated under stirring for 24 h with the high power LED (440 nm ± 10 nm, 3 Watts electrical power, 20 lumen, 700 mA, LED 3W 3 STAR LB BL ZXHL-LBBC LUXEON). For analytic monitoring, 500 µL of the reaction mixture were taken out by an Eppendorf pipette and mixed with 500 µL of toluene as internal standard. 1 µL of this solution was analyzed by GC or GC/MS.

General procedure for the kinetic monitoring of the photoreduction of nitrobenzene

Triethanolamine (TEOA, 300 mg, $2 \cdot 10^{-3}$ mol), nitrobenzene ($2 \cdot 10^{-4}$ mol), $PbPnO_2X$ (50 mg) and 2.5 mL of acetonitrile were placed in the reaction vial, sealed with a septum and cooled by liquid nitrogen. The mixture was allowed to warm up to room temperature under 50 mbar and flushed with nitrogen. This procedure was repeated one time, afterwards the cell was irradiated under stirring for 24 h with the high power LED (440 nm ± 10 nm, 3 Watts electrical power, 20 lumen, 700 mA, LED 3W 3 STAR LB BL ZXHL-LBBC LUXEON). For kinetic monitoring, 20 µL of the reaction mixture were taken out directly by a Hamilton syringe and mixed with 20 µL of toluene as standard. 1 µL of this solution was analyzed by GC.

2.4.4 Determination of the Flat Band Potentials

The sample (50 mg) was sonicated for 15 min in an aqueous 0.1 mol/L solution of KNO_3. Further, one drop of concentrated HNO_3 was added to this dispersion. Subsequent, 10 mg of methylviologen, a dicationic spicy with a pH-independent redox-potential,[18] were added to the mixture. The dispersion was stirred under nitrogen-atmosphere to avoid quenching of the photochemical reaction due to oxygen. A platinum electrode, an Ag/AgCl-reference-electrode and a pH-meter were attached to determine the dispersion's potential and pH-value, respectively. In a next step, this setup was irradiated with a 150 W Xe arc light source for 60 min. After this time, pH and potential were recorded. Then, the pH was increased by adding NaOH at various concentrations drop wise. The changes in pH and potential were recorded

subsequently after the equilibrium-state was reached. The obtained experimental data were used to derive the flat band potentials according to ref..[18,19]

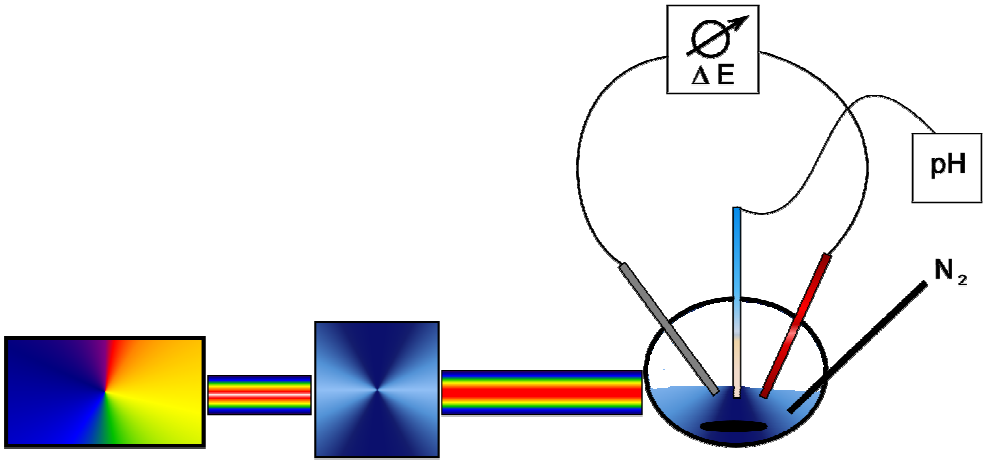

Fig. 1: Schematic setup for the measurement of the flat band potential by using a Xe arc light source, a separate IR-filter is required.

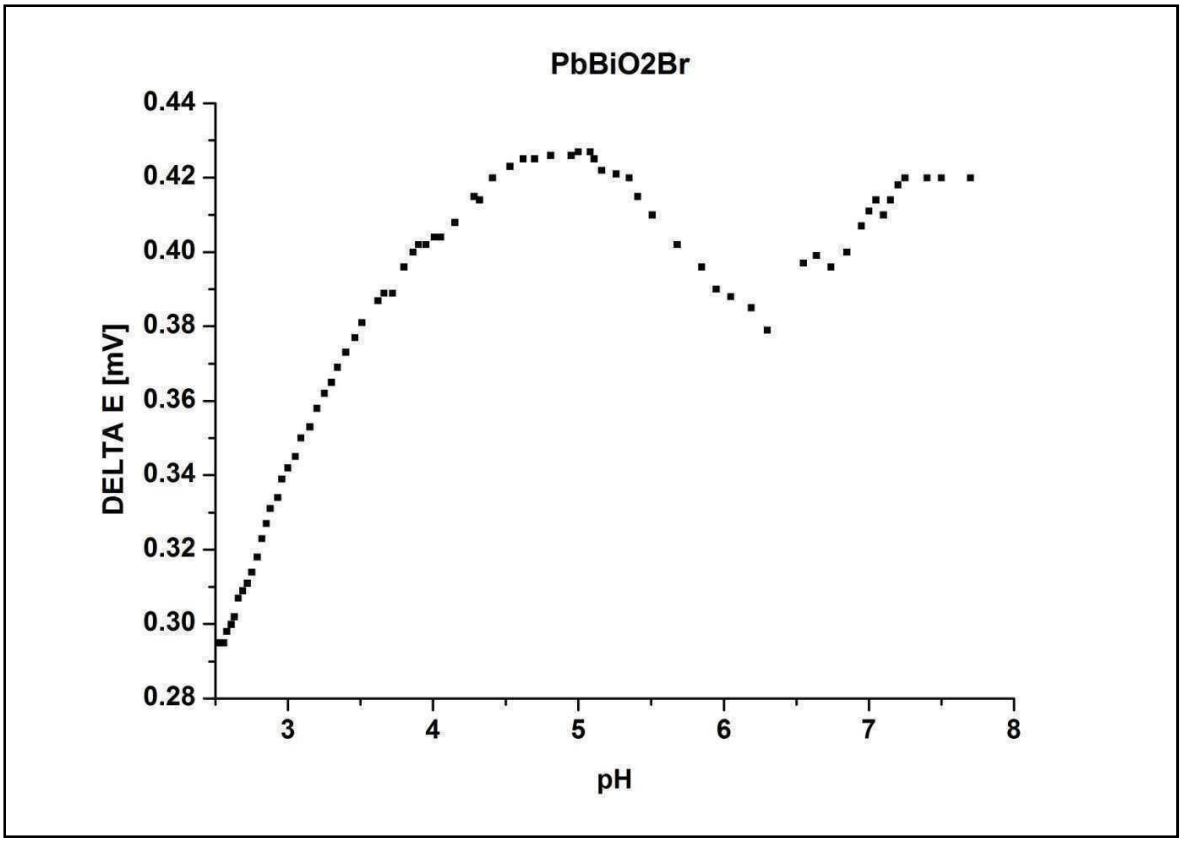

Fig. 2a: Titration curve of $PbBiO_2Br$ under the mentioned conditions above.

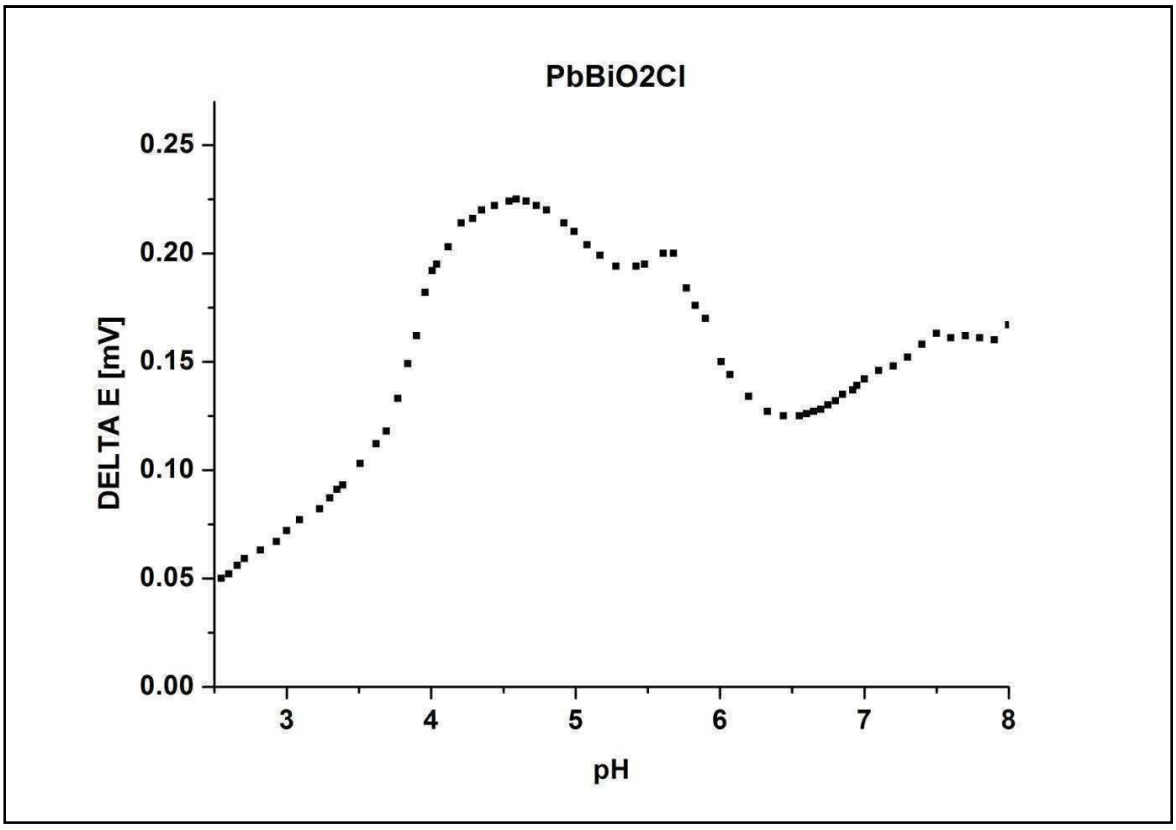

Fig. 2b: Titration curve of $PbBiO_2Cl$ under the mentioned conditions above.

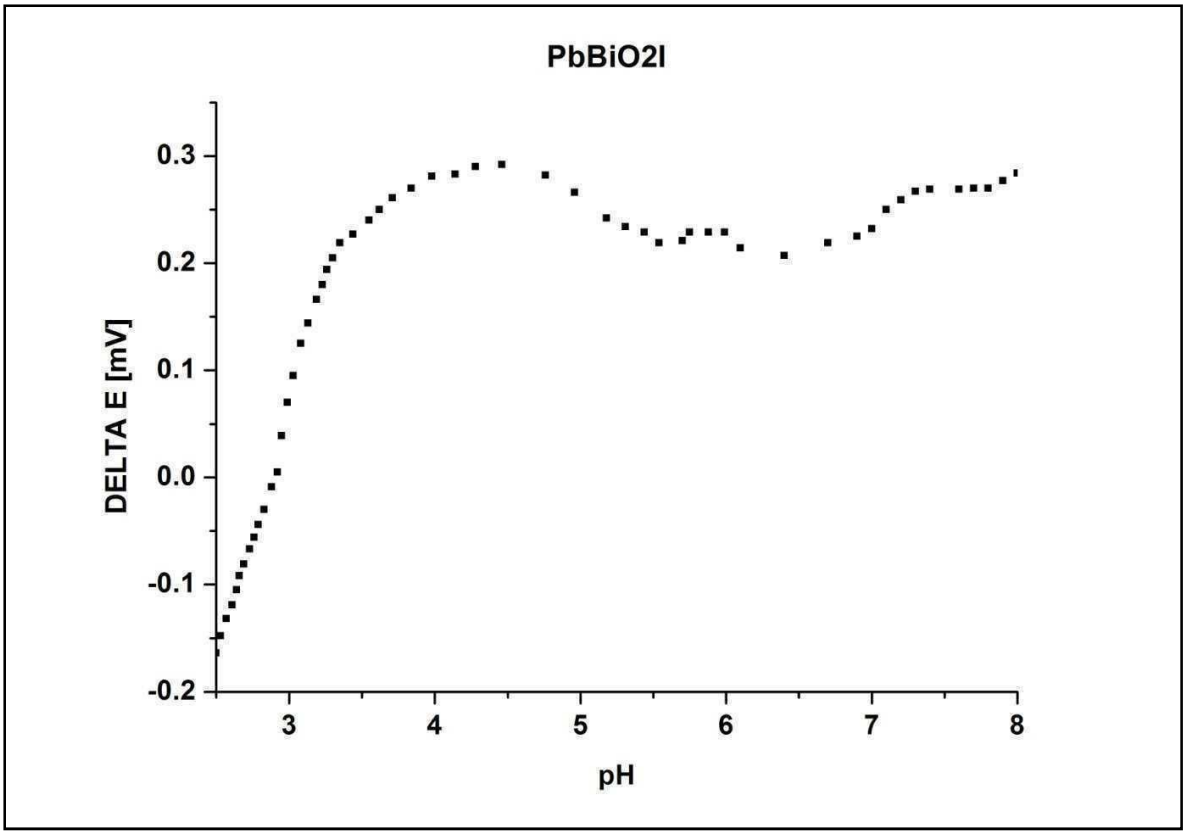

Fig. 2c: Titration curve of $PbBiO_2I$ under the mentioned conditions above.

2.5 References

[1] S. Westenhoff, I. A. Howard, J. M. Hodgkiss, K. R. Kirov, H. A. Bronstein, C. K. Williams, N. C. Greenhorn, R. H. Friend, *J. Am. Chem. Soc.* **2008,** *130,* 13653-13658.

[2] S. Rau, B. Schäfer, D. Gleich, E. Anders, M. Rudolph, M. Friedrich, H. Görls, W. Henry, J. G. Vos, *Angew. Chem.* **2006,** *118,* 6361-6364.

[3] D. A. Nicewicz, D. W. C. MacMillan, *Science* **2008,** *322,* 77-80.

[4] J. M. R. Narayanam, J. W. Tucker, C. R. J. Stephenson, *J. Am. Chem. Soc.* **2009,** *131,* 8756-8757.

[5] S. O. Flores, O. Rios-Bernji, M. A. Valenzuela, I. Crdova, R. Gmez, R. Gutirrez, *Topics in Catalysis* **2007,** *44,* 507-511.

[6] (a) S. Füldner, R. Mild, H. I. Siegmund, A. J. Schroeder, M. Gruber, B. König, *Green Chemistry* **2010,** *12,* 400-406. (b) M. Zhang, C. Chen, W. Ma, J. Zhao, *Angew. Chem.* **2008,** *120,* 9876-9879.

[7] C. Radhakrisham, M. K. F. Lo, M. V. Warrier, M. A. Garcia-Garibay, H. G. Monbouquette, *Langmuir* **2006,** *22,* 5018-5024.

[8] (a) A. Pfitzner, P. Pohla, *Z. Anorg. Allg. Chem.* **2009,** *635,* 1157-1159. (b) Z. Shan, W. Wang, X. Lin, H. Ding, F. Huang, *J. Solid State Chem.* **2008,** *181,* 1361-1366.

[9] R. Brosius, D. Gammon, F. Van Laar, E. Van Steen, B. Sels, P. Jacobs, *J. Catal.* **2006,** *239,* 362-368.

[10] (a) H. Tada, A. Takao, T. Akita, K. Tanaka, *ChemPhysChem* **2006,** *7,* 1687-1691. (b) Y. Matsushita, S. Kumada, K. Wakabayashi, K. Sakeda, T. Ichimura, *Chem. Lett.* **2006,** *35,* 410-411. (c) H. Tada, T. Ishida, A. Takao, S. Ito, S. Mukhopadhay, T. Akita, K. Tanaka, H. Kobayashi, *ChemPhysChem* **2005,** *6,* 1537-1543.

[11] P. Pohla, *Dissertation* **2010,** Universität Regensburg.

[12] H. An, Y. Du, T. Wang, C. Wang, W. Hao, J. Zhang, *Rare Metals* **2008,** *27,* 243-250.

[13] Y. Chen, S. Yan, K. Wan, L. Lou, *J. Photochem. Photobiol. A: Chem.* **2005,** *6,* 1537-1543.

[14] U. Singh, S. Verma, H. N. Ghosh, M. C. Rath, K. I. Priyadarsini, A. Sharma, *J. Mol. Catal. A.: Chem.* **2010,** *318,* 106-111.

[15] Activation of band gap decreasing has been excluded by UV-Vis spectra, which is contrary to the reported photo catalysis with BiOCl.

[16] K. Schwetlick, *Organikum* **2001,** Wiley-VCH.

[17] *STOE WINX^{POW}*, Version 1.08 (16-Nov-2000), STOE & Cie GmbH, Darmstadt, **2000**.

[18] A. M. Roy, G. C. De, N. Sasmal, S. S. Bhattacharyya, *International Journal of Hydrogen Energy* **1995**, *20*, 627.

[19] (a) A. M. Roy, G. C. De, N. Sasmal, S. S. Bhattacharyya, *Int. J. Hydrogen Energy* **1995**, *20*, 627. (b) O. L. Stroyuk, O. Y. Rayevska, A. V. Kozytskiy, S. Y. Kuchmiy, *J. Photochem. Photobiol. A: Chemistry* **2010**, *210*, 209.

3 Heterogeneous Organophotocatalysis - Visible-Light-Induced α-Alkylations of Aldehydes via unmodified TiO_2

3.1 Introduction

Developing efficient and economical *C-C* bond formations is an important challenge in current organic syntheses. Transition metal catalyzed C-C-bond forming reactions, like Stille-, Sonogashira- and Suzuki-couplings, have been developed widely.[1] Enolate based chemistry, for example with the Evans-auxiliary[2] or Enders SAMP-RAMP-method[3] allow the stereoselective alkylation of C-H acidic compounds. More recent, organocatalysis has found a wide range of applications in *C-C* bond formation in organic synthesis.[4] Organophotocatalyses use visible light and may be therefore very efficient in terms of energy consumption. The first enantioselective organophotoredox α-alkylation of aldehydes was reported by MacMillans et al.. They used imidazolidinone as organocatalyst and $[Rubpy_3]Cl_2 \cdot 6H_2O$ as photoredox catalyst.[5] Furthermore, the principle of single-electron-transfer (SET) initiated by an excited ruthenium complex has been successfully applied to the radical cyclisation of indol and pyrrole derivatives[6] and to the oxidative Aza-Henry-reaction of tertiary amines as 1,2,3,4-tetrahydroisoquinoline and pyrrolidine derivatives (Scheme 1).[7]

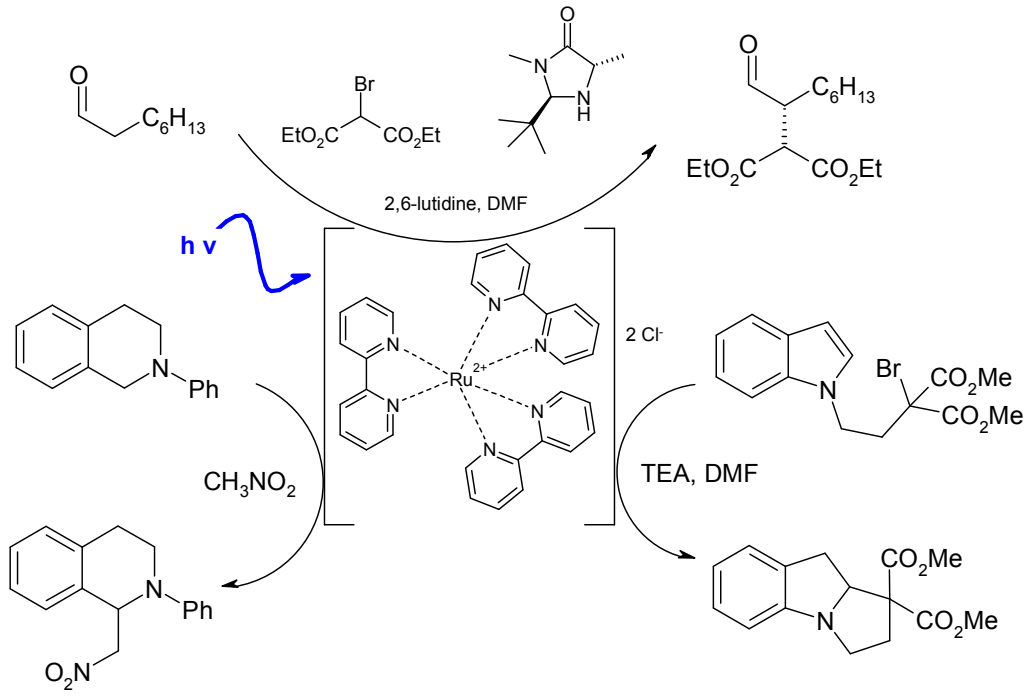

Scheme 1. Examples of SET-reactions as (a) α-alkylation of octanal, (b) radical cyclisation of indol and (c) Aza-Henry-reaction of 1,2,3,4-tetrahydroisoquinoline.

The reactions utilize light energy, but still lack from several disadvantages: The photocatalyst absorbs only in the blue region of the solar spectrum, transition metals as iridium or ruthenium are required, which are toxic, expensive and of limited availability, and separation of the catalyst after the reaction may cause difficulties. Organic photoredoxcatalyst, like have been investigated for the enantioselective α-alkylation by Zeitler *et al.*[8] The photosensitizers absorb in the visible solar region up to 530 nm and catalyze the reactions efficiently. However, for simple reuse of the photocatalyst and the development of continuous processes heterogeneous photocatalysts are required. Semiconductors, such as TiO_2 or CdS may therefore be a valuable alternative. We report here the use of unmodified TiO_2 (P25, Degussa), a cheap and commercial available semiconductor with a high surface area (50 mg = 2 m^2) as photocatalyst in redox organocatalysis. Visible-light absorption has been achieved by charge transfer complexations of aldehydes on the surface of TiO_2; a principle which has been reported for titania and organic substrates as catechol (Scheme 2). [7]

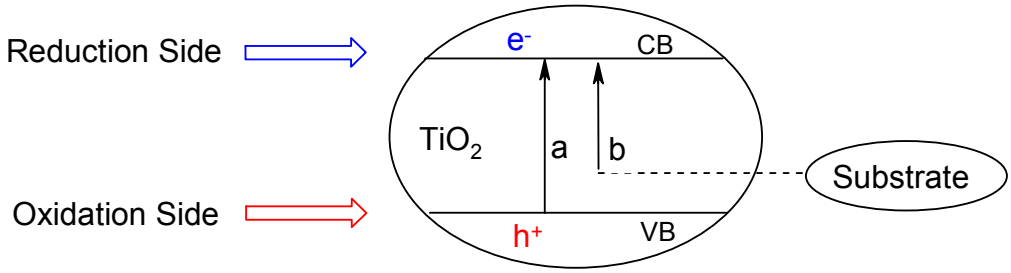

Scheme 2. Principle of the redox active semiconductor TiO_2 and (a) the UV light absorption (365 nm) as an unmodified sample and (b) Vis light absorption (> 400 nm) with charge transfer complexes.

3.2 Results and Discussions

Irradiation in the band gap of TiO_2 (365 nm) usually leads to unselective degradations of organic substrates, which could be inhibited by irradiation with visible light. Therefore, dye-sensitization and doping of TiO_2 with transition metals or nitrogen, sulfur or carbon have been applied. Charge-transfer-complexations have been investigated with SO_3 or catechol which physically adsorbed at the surface of TiO_2 increase significantly the absorption in the visible-light region of 410 - 500 nm. Octanal and hydrocinnamaldehyde, starting materials of the α-alkylations, have shown similar effects: Unmodified TiO_2 (Degussa P25) absorpsn up to 405 nm, whereas octanal treated TiO_2 showed significant higher absorption wavelenghts until 450 nm (Figure 2). Adsorbed 2,6-lutidine only shifted the absorption to 410 nm and 2-bromo diethylmalonate did not influence TiO_2 absorption properties at all. The increased absorption in case of octanal might be due to the mentioned charge-transfer-complexations.

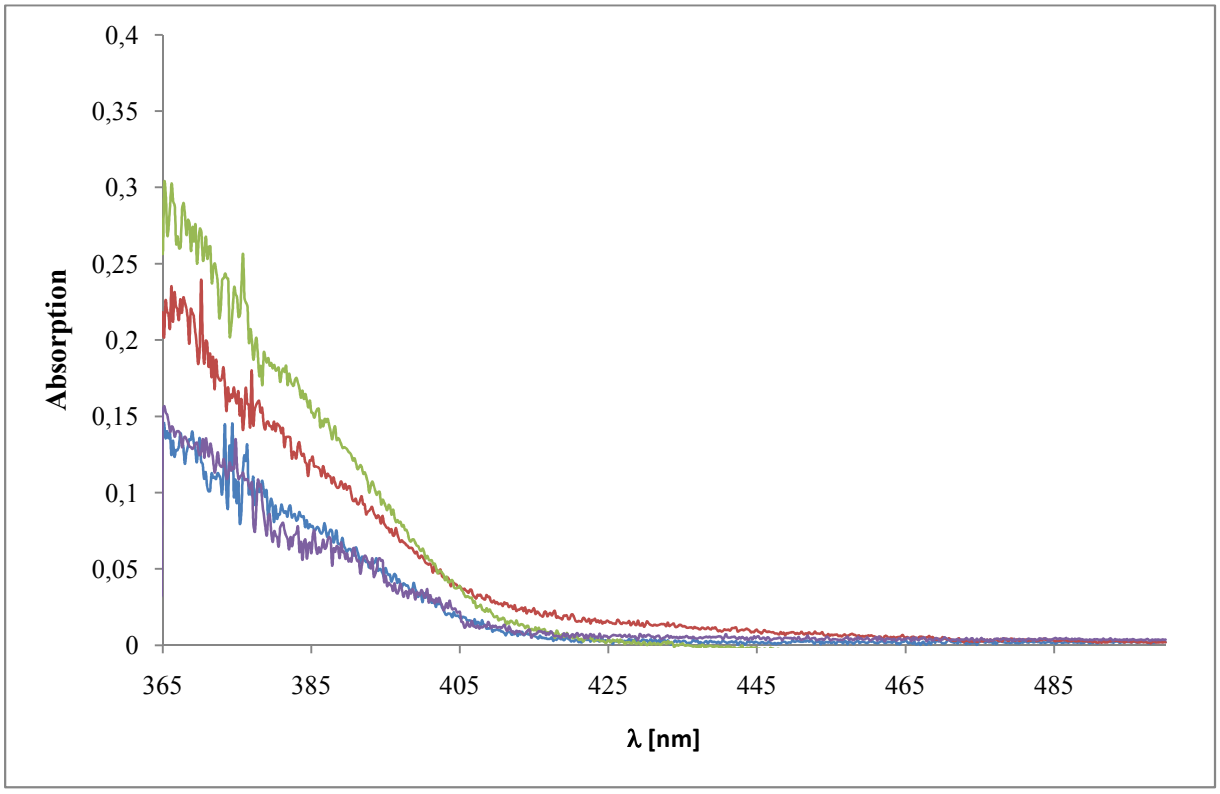

Fig. 2: Absorption spectra of (a) blanc TiO_2 (blue), (b) 2-bromo diethylmalonate on TiO_2 (violet), (c) octanal on TiO_2 (red) and (d) 2,6-lutidine on TiO_2 (green).

Preliminary, the photoredox α-alkylation of octanal with 2-bromo diethylmalonate and TiO_2 has been investigated in different solvents, because of the known solvent dependence of the

TiO_2 photocatalytic activity.[9] 2-Bromo diethylmalonate has been chosen as alkylation reagent due to its high radical stability.

Table 1. Conversion of photocatalytic α-alkylation of octanal in different solvents.

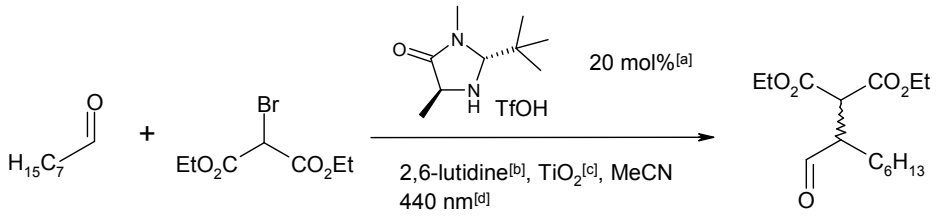

Entry	Solvent	Yield [%][e]
1	DMSO	-
2	DMF	40
3	MeCN	80

[a] Related to 2-bromo diethylmalonate. [b] 2 Equivalents related to 2-bromo diethylmalonate. [c] 50 mg. [d] High power LED 3 Watts electric power, 80 lumen, emission wavelength 440 +/- 10 nm. [e] Determined from the integration of signals in gas chromatogram with an internal standard.

Table 2. Determination of the optimum amount of TiO_2 photocatalyst in reaction vials.

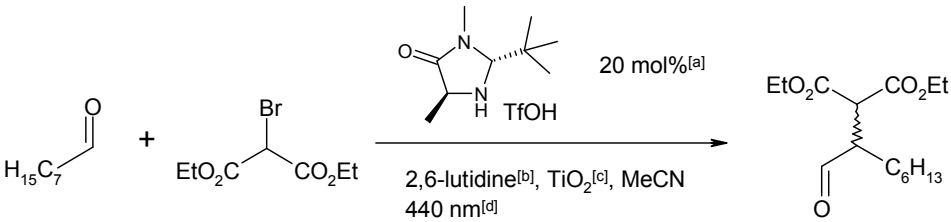

Entry	m_{TiO2} [mg][c]	P_{el} [mW][e]	Yield [%][f]
1	-	22.4	-
2	10	10.0	-
3	20	5.9	-
4	30	2.1	25
5	40	0.7	49
6	50	-	79
7	60	-	72
8	70	-	69
9	100	-	28

[a] Related to 2-bromo diethylmalonate. [b] 2 Equivalents related to 2-bromo diethylmalonate. [c] P25 from Degussa. [d] High power LED 3 Watts electric power, 80 lumen., emission wavelength 440 +/- 10 nm. [e] See literature, standard reaction vial has been taken instead of the standard cuvette.[10] [f] Determination from integration of the signals in gas chromatogram and calculation with an internal standard.

Acetonitrile as solvent gave the highest conversions and yields of 80 % compared to DMF with 40 % and DMSO with no conversion (Table 1): increased solvents polarity lead to decreased yields.[11] The reaction conditions were optimized regarding the amount of catalyst, the reaction temperature and the irradiation wavelength. The optimum amount of TiO_2 was determined by maximum light absorption depending on the maximum yield (Table 2). Therefore, the reaction solutions have been irradiated in the reaction vials with different amounts of TiO_2 and the yields after the reaction and light absorption during the irradiations have been measured. Maximum yields of 80 % of diethyl 2-(1-oxooctan-2-yl)malonate have been obtained when 50 mg of photocatalyst were used and maximum light absorption was achieved (Table 2, Entry 6).

Table 3. α-Alkylation of octanal with 2-bromo diethylmalonate under different conditions.

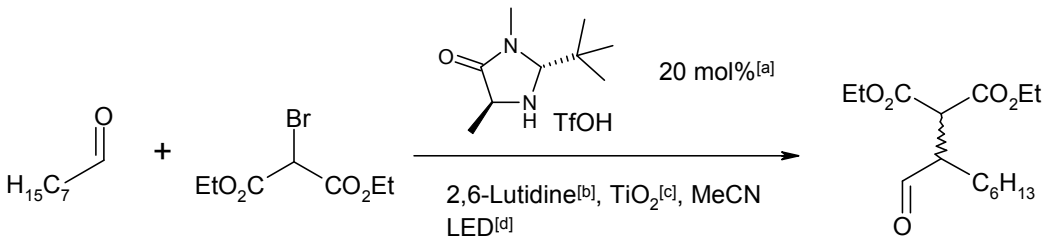

2 equival.

Entry	λ [nm][d]	T [°C]	Irradiation Time [h]	Yield [%][e]	*ee* [%][f]
1	440	40	13	80	71
2	440	-10	20	87	85
3	400	40	5	75	68
4	400	-10	12	78	75

[a] Related to 2-bromo diethylmalonate. [b] 2 Equivalents related to 2-bromo diethylmalonate. [c] P25 from Degussa. [d] LED 400 nm +/- 10 nm: 1 Watt electric power, 30 lumen, LED 440 nm +/- 10 nm: 3 Watts electric power, 80 lumen. [e] After workup and chromatography. [f] Determination from integration of the signals of the diastereomeres from acetalisation in ^{1}H-NMR spectrum.

Irradiation with shorter wavelengths as 400 nm lead to faster conversions but lower yields compared to irradiation with 440 nm under identical reaction temperatures (Table 3, Entries 1 and 3, 2 and 4). TiO_2 light absorption at 400 nm has been significant higher as for light of 440 nm as it has been already shown in Figure 2, which explained the enhanced reaction times. Lower temperatures lead to higher yields and *ee* values: (a) 80 % yield and 71 % *ee* for 40 °C and 87 % yield and 85 % *ee* for -10 °C at 440 nm and (b) 75 % yield and 68 % *ee* for 40 °C and 78 % yield and 75 % *ee* for -10 °C at 400 nm. This effect has already been reported for homogeneous photoredox catalysis with organic dyes,[8] asymmetric organocatalysis,[12]

asymmetric Diels-Alder reactions[13] and enantioselective Broensted acid catalyzed enamine Mannich reactions.[14]

Table 4. α-Alkylations of octanal and hydrocinnamaldehyde at different wavelengths and with different substrates at -10 °C.

			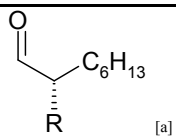 [a]		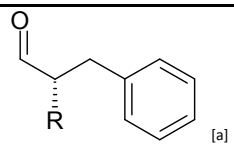 [a]	
Entry	**Substrate R-Br**	**λ [nm][b]**	**Irradiation Time [h]**	**Yield [%][c]**	**Irradiation Time [h]**	**Yield [%][c]**
1	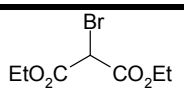	440	20	87	24	85
2		400	12	78	12	80
3	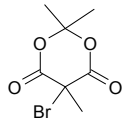	440	24	-	-	-
4		400	24	-	-	-
5	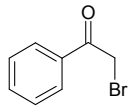	440	24	9	24	8
6		400	24	11	24	12
7	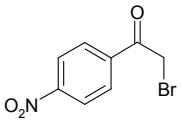	440	24	10	24	7
8		400	24	12	24	4
9	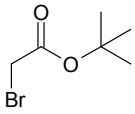	440	24	-	24	-
10		400	24	-	24	-
11	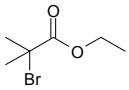	440	24	-	24	-
12		400	24	-	24	

[a] Standard conditions as in case of 2-bromo diethylmalonate at -10 °C. [b] LED 400 nm +/- 10 nm: 1 Watt electric power, 30 lumen, LED 440 nm +/- 10 nm: 3 Watts electric power, 80 lumen. [c] Determination from integration of the signals in gas chromatogram and calculation with an internal standard, work up and *ee* determination only in cases of 2-bromo diethylmalonate and octanal and hydrocinnamaldehyde.

Hydrocinnamaldehyde and several radical precursors have been investigated under the optimized reaction conditions, too (Table 4). All reactions have been investigated at -10 °C and different irradiation wavelengths, but only 2-bromo diethylmalonate has been added successfully to octanal and hydrocinnamaldehyde with yields of 87 % and 85 % *ee* (440 nm) for octanal and 85 % and 79 % *ee* (440 nm) for hydrocinnamaldehyde (Table 4, Entries 1 and 2). Substituted and non-substituted 2-bromo acetophenones have been investigated for the photocatalytic substitution to octanal and hydrocinnamaldehyde, but yields did not exceed 12

% (Table 4, Entries 3 - 6). The observation is surprising, as the alpha radicals of acetophenone (BDE = 90 kcal/mol) and diethylmalonate (BDE = 93 kcal/ mol) are of very similar stabilities.[15] Moreover, physical adsorption seemed to play a more important role, which has been reported to be weak for acetophenone on the surface of TiO_2[16] compared to aniline,[17] sulphuric acid containing polyaromatics[18] and carboxylic acids.[19] Furthermore, a certain distance is required for a productive electron transfer from TiO_2 to the substrate, which seemed to be matched for 2-bromo diethylmalonate, but not for α-bromo acetophenones.[16] Similar radical stability in alpha- positions has been known for mono esters as ethyl α-bromoisobutyrate (BDE = 92.7 kcal/ mol) and a little higher for *tert*-butyl bromoacetate (BDE = 96.1 kcal/ mol).[15] Similar adsorption effects have been reported for transesterfications over titanosilicate molecular sieves of diethylmalonate.[20] Here, titania has to be found the active catalyst containing Lewis acid sites and no Brönsted sites and only linear esters with two carbonyl groups as ethylacetoacetate and diethylmalonate have been transesterficated. Mono esters and cyclic esters as dimethyl carbonate failed. These observations may indicate a reason why *cycl*-isopropylidene 1-bromo-methylmalonate failed in the reaction to give α-alkylated octanal or hydrocinnamaldehyde.

Furthermore, photoredox dehalogenations have been investigated with TiO_2 to see if an electron transfer is possible from this semiconductor to the α-bromo acetophenones (Table 5).

Table 5. Photocatalytic dehalogenations of α-bromo acetophenones.

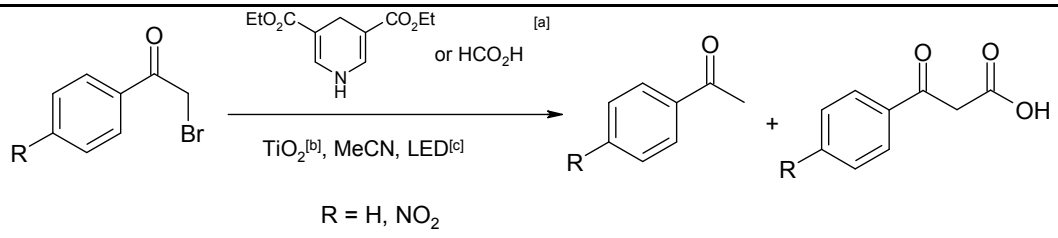

Entry	R	λ [nm][c]	Yield acetophenone [%][d]
1	H	400	-
2	H	440	-
3	NO_2	400	-
4	NO_2	440	-

[a] 1.1 Equivalent related to the α-bromo acetophenone. [b] 50 mg. [c] LED 400 nm +/- 10 nm: 1 Watt electric power, 30 lumen, LED 440 nm +/- 10 nm: 3 Watts electric power, 80 lumen. [d] Determination from integration of the signals in gas chromatogram and calculation with an internal standard.

Only starting materials have been obtained when the Hantzsch ester was used as hydride source and β-ketocarboxylic acids have been observed when using formic acid. A photocatalytic effect was excluded by stepwise omitting irradiation and TiO_2 still leading to the same β-ketocarboxylic acids. These transformations have been known for acetophenones and CO_2 under basic conditions,[21] which are very similar to our conditions where formic acid acted as CO_2 source and DIPEA as base. Additionally, no ethyl isobutyrate and no *tert*-butyl acetate have been obtained, when ethyl α-bromoisobutyrate and *tert*-butyl bromoacetate have been investigated under identical photocatalytic conditions as the α-bromo acetophenones.
Similar radical stabilities of acetophenone, diethylmalonate and the mono esters, different adsorption affinities onto the surface of TiO_2 and no photo dehalogenations of the α-bromo acetophenones and mono esters indicate the importance of two activating carbonyl groups in the radical precursors with the right geometry for an attractive interaction to the surface of TiO_2.

3.3 Conclusion

Stereoselective semiconductor photocatalysis was achieved by the combination of unmodified TiO_2 and a MacMillan catalyst. α-Alkylations of octanal and hydrocinnamaldehyde with 2-bromo diethylmalonate resulted in high product yields and good stereoselectivity under reduced temperatures.

Furthermore, several other radical precursors have been investigated towards heterogeneous photoredox α-alkylations of aldehydes. Similar radical stabilities of the bromo compounds, no dehalogenation reactions for the mono carbonyl substances acetophenones and esters indicate sensitive surface-interaction-effects of TiO_2. However, theses enantioselective *C-C* bond formations should be further investigated with several functionalized diesters to understand electronic and steric effects of the precursors on the radical process.

3.4 Experimental Part

3.4.1 General methods

Unless otherwise noted, all commercially available compounds were used as provided without further purification.

NMR spectra were recorded on a Bruker Avance 300 (300.13 MHz) using the solvent peak as internal reference ($CDCl_3$: _ H 7.26; _ C 77.0). Multiplicities are indicated, s (singlet), d (doublet), t (triplet), q (quartet), quint (quintet), sept (septet), m (multiplet)); coupling constants (*J*) are in Hertz (Hz). All reactions were monitored by thin-layer chromatography using Merck silica gel plates 60 F254;

visualization was accomplished with UV light and/or staining with appropriate stains (anisaldehyde or $KMnO_4$ solutions). Standard chromatography procedures were followed (particle size 63-200 μm).

A GC 5890 Series II from Hewlett-Packard was used. Injection-temperature (split injection: 40:1 split) was at 50 °C, detection temperature was at 300 °C (FID). The column was a capillary column was a capillary column from J+W Scientific - DB-5MS / 30 m X 0.25m / 0.25 μm film. Helium was used as carrier gas with a low of 1 mL/ min. Data acquisition and evaluation was done by using the software Agilent ChemStation Rev.A.06.03. (509).

All reactions were carried out under a protective atmosphere of dry nitrogen using oven-dried glassware unless otherwise stated.

Irradiation with green light was performed using high-power LEDs: LUXEON LED Star LXHL-LB3C, 447 nm, 3 Watt, 30 Lumen @ 1000 mA) for reactions at normal and decreased temperatures; CREE XL 7090UVV-L100-0001 R, 400 nm, 1.23 Watt, 1000mA) for reactions at normal and decreased temperatures.

3.4.2 Photoreactions

3.4.2.1 Dehalogenations of α-bromo acetophenones

General procedure for analytical scale

α-Bromo acetophenone (0.39 mmol), DIPEA (μL, 0.78 mmol), Hantzsch ester (19 mg, 0.45 mmol) or HCO_2H (33 μL, 0.45 mmol), TiO_2 (50 mg) and 2.5 mL MeCN (abs.) were placed in the reaction vial, sealed with a rubber septum and cooled with liquid nitrogen. The mixture was allowed to warm up to room temperature under 50 mbar and flushed with nitrogen. This

procedure was repeated once and the reaction vial was irradiated under stirring for a certain time with the LED.

For analyzing, 100 µL of the reaction mixture were taken out directly by Eppendorf pipette and mixed with 900 µL MeCN. 1 µL of this solution was injected in the GC. The signals were integrated from the chromatogram.

3.4.2.2 α-Alkylations of aldehydes

General procedure on analytical scale

The halogen compound (0.39 mmol), octanal (120 µL, 0.78 mmol), 2,6-lutidine (90 µL, 0.78 mmol), MacMillan-catalyst (16 mg, 0.078 mmol), TiO_2 (50 mg), chlorobenzene (0.39 mmol) and 2 mL MeCN (abs.) were placed in the sample vial, sealed with a septum and frozen with liquid nitrogen. The mixture was allowed to warm up to room temperature under 50 mbar and flushed with nitrogen. This procedure was repeated once and the cell was irradiated under stirring for the given time with the LED.

For analyzing, 100 µL of the reaction mixture were taken out directly by Eppendorf pipette and mixed with 900 µL MeCN. 1 µL of this solution was injected in the GC. The signals were integrated from the chromatogram.

General procedure on preparative scale

The halogen compound (0.78 mmol), octanal (305 µL, 1.95 mmol), 2,6-lutidine (182 µL, 1.56 mmol), MacMillan-catalyst (33 mg, 0.156 mmol), TiO_2 (50 mg), chlorobenzene (0.78 mmol) and 2.5 mL MeCN (abs.) were placed in the sample vial, sealed with a rubber septum and frozen with liquid nitrogen. The mixture was allowed to warm up to room temperature under 50 mbar and flushed with nitrogen. This procedure was repeated once and the cell was irradiated with the LED under stirring.

After the reaction TiO_2 was filtered over celite, the filter cake washed with 3x 10 mL Et_2O, the organic layers extracted with 2x 20 mL water and the water phase re-extracted with 3x 10 mL Et_2O. The united organic layers were extracted with 1x 10 mL NH_4Cl-, 1x 10 mL $NaHCO_3$- and 1x 10 mL NaCl-solution, dried over $MgSO_4$ and evaporated to dryness. The yellow residue was purified by column chromatography at silica gel (PE/Et_2O 6:1) and the enantiomeric colorless oils checked by ^1H-/^{13}C-NMR-spectroscopy.

The alkylated octanal (20 mg) was dissolved in 5 mL of abs. DCM, 10 mg of (*2S,4S*)-(+)-pentanediol and 1 mg of *p*TsOH were added and the solution stirred for 5 h under a nitrogen

atmosphere. DCM was evaporated, the residue dissolved in 800 µL of $CDCl_3$ and checked by ^{1}H-NMR-spectroscopy. The enantiomeric excess was determined by integration of the ^{1}H-NMR resonance signals for the C**H**(EWG) of the acetals.

3.4.3 GC analyses of photoreactions

Chlorobenzene has been used as internal standard within the photoreactions. Calibration curves have been measured for octanal, hydrocinnamaldehyde, 2-bromo diethylmalonate and 2,6-lutidine (Figure 2). A GC 5890 Series II from Hewlett-Packard was used. Injection-temperature (split injection: 40:1 split) was at 50 °C, detection temperature was at 300 °C (FID). The column was a capillary column was a capillary column from J+W Scientific - DB-5MS / 30 m X 0.25m / 0.25 µm film. Helium was used as carrier gas with a low of 1 mL/ min. Data acquisition and evaluation was done by using the software Agilent ChemStation Rev.A.06.03. (509).

GC-measurements were made and investigated while integrating the signals obtained. The GC oven temperature program adjustment was as follows: The initial temperature was 40 °C. This was kept for 3 minute and then increased constantly at a rate of 15 °C/min for 16 minutes. The final temperature of 280 °C was kept for 5 minutes.

3.4.4 Experimental data for the synthesis of precursors and α-alkylation of aldehydes

***Cycl*-isopropylidene 1-bromo-methylmalonate (1)**

SF 308c

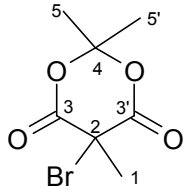

1

According to literature[22] NaF (600 mg, 14.2 mmol) and *cycl*-isopropylidene methylmalonate (750 mg, 4.74 mmol) were dissolved in 15 mL of dry $CHCl_3$ in a heated and evacuated 3-necked-100 mL flask under nitrogen atmosphere. The reaction mixture was heated to 55 °C and a solution of bromine (300 µL, 5.7 mmol) in 15 mL of $CHCl_3$ was added drop wise to the mixture in 2 h and further refluxed for 1 h. The solution was allowed to cool to room

temperature, the solid filtered and the filtrate evaporated to dryness. The remaining oil was crystallized from 10 mL of *n*-hexane, the colorless solid filtered, crystallized from 10 mL of *i*PrOH and dried at high vacuum to give 450 mg (yield: 40 %, Lit.[22]: 73 %) of a colorless solid.

$C_7H_9BrO_4$

M = 237 g/mol.

^{1}H NMR (300 MHz, $CDCl_3$, 25 °C, TMS): δ = 1.77 (s, 3 H, 1-H), 2.00 (s, 3 H, 5-H), 2.19 (s, 3 H, 5'-H).

^{13}C NMR (75 MHz, $CDCl_3$): δ = 25.5 (q, C-1), 26.7 (q, C-5), 29.3 (q, C-5'), 41.4 (s, C-2), 106.9 (s, C-4), 164.7 (s, C-3/3').

(*R*)-Diethyl 2-(1-oxooctan-2-yl)malonate (2)

SF 295a

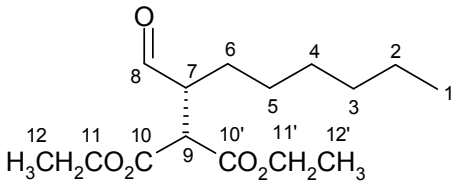

2

According to the general procedure on preparative scale the reaction mixture was irradiated for 20 h at -10 °C with 440 nm and worked up and purified by column chromatography as described to give 87 % yield, 85 % *ee* of a colorless oil. Enantiomeric excess was determined after acetalisation of the aldehyde with (2*S*, 4*S*)-(+)-pentanediol via integration of ^{1}H-NMR-signals of the diastereomeric acetals ($CDCl_3$, both doublets) at 3.68 ppm (minor) and 3.58 ppm (major).

$C_{15}H_{26}O_5$

M = 286.16 g/mol.

R_f = 0.32 (PE/ Et_2O 6:1).

^{1}H NMR (300 MHz, $CDCl_3$, 25 °C, TMS): δ = 0.85- 0.91 (m, 3 H, 1-H), 1.25-1.46 (m, 6 H, 12/12'-H), 1.56-1.76 (m, 14 H, 1/2/3/4/5/6-H), 3.06-3.14 (m, 1 H, 7-H), 3.72 (d, *J* = 8.6 Hz, 1 H, 9-H), 4.15-4.30 (m, 4 H, 11/11'-H), 9.75 (d, *J* = 8.6 Hz, 1 H, 8-H).

^{13}C NMR (75 MHz, $CDCl_3$): δ = 14.0 (q, C-1), 14.1 (q, C-13/13'), 22.5 (t, C-2), 26.4 (t, C-3), 27.0 (t, C-4), 29.3 (t, C-5), 31.4 (t, C-6), 50.3 (d, C-8), 51.8 (d, C-10), 61.8 (t, C-12/12'), 168.1 (s, C-11/11'), 201.6 (s, C-9).

(*R*)-Diethyl 2-(1-oxo-3-phenylpropan-2-yl)malonate (3)

SF 299a

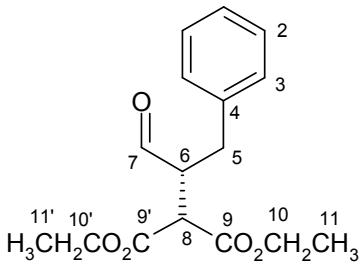

3

According to the general procedures on preparative scale: After irradiation with a LED 400 nm or 440 nm for 18 hours at -10 °C the reaction was worked up and purified by column chromatography as described to give 85 % yield, 79 % *ee* of a colorless oil. Enantiomeric excess was determined after acetalisation of the aldehyde with (2*S*, 4*S*)-(+)-pentanediol via integration of ^{1}H-NMR-signals of the diastereomeric acetals ($CDCl_3$, both doublets) at 4.81 ppm (minor) and 4.92 ppm (major).

$C_{16}H_{20}O_5$

M = 292.17 g/mol.

R_f = 0.25 (PE/ Et_2O 6:1).

^{1}H NMR (300 MHz, $CDCl_3$, 25 °C, TMS): δ = 1.27 (t, *J* = 4.9 Hz, 6 H, 11/11'-H), 2.83 (dd, *J* = 7.3, 14.1 Hz, 1 H, 5a-H), 3.12 (dd, *J* = 7.5, 14.1 Hz, 1 H, 5b-H), 3.39 (q, *J* = 7.3 Hz, 1 H, 6-H), 3.68 (d, *J* = 7.3, 14.2 Hz, 1 H, 8-H), 4.17-4.22 (m, 4 H, 10/10'-H), 7.18-7.32 (m, 5 H, 1/2/2'/3/3'-H), 9.73 (d, *J* = 7.3 Hz, 1 H, 7-H).

^{13}C NMR (75 MHz, $CDCl_3$): δ = 14.0 (q, C-11/11'), 33.2 (t, C-5), 51.5 (d, C-6), 55.9 (d, C-8), 62.0 (t, C-10/10'), 126.9 (d, C-1), 128.2 (d, C-2/2'), 129.4 (d, C-3/3'), 137.4 (s, C-4), 167.9 (s, C-9), 201.1 (s, C-7).

3.4 References

[1] (a) A.B. Dounay, L.E. Overman, *Chem. Rev.* **2003,** *103,* 2945-2963. (b) Y. Shi, S.M. Peterson, W.W. Haberaecker III, S.A. Blum, *J. Am. Chem. Soc.* **2008,** *130,* 2168-2169. (c)

[2] D.A. Evans, K.A. Scheidt, J.N. Johnston, M.C. Willis, *J. Am. Chem. Soc.* **2001,** *123,* 4480-4491.

[3] K.G. Avenport, H. Eichenauer, D. Enders, M. Newcomb, D.E. Bergbreiter, *J. Am. Chem. Soc.* **1979,** *101,* 5654-5659.

[4] (a) A. Berkessel, H. Gröger, *Asymmetric Organocatalysis,* WILEY-VCH, Weinheim, **2005;** (b) A. Dondoni, A. Massi, *Angew. Chem.* **2008,** *120,* 4716-4739.

[5] D.A. Nicewicz, D.W.C. MacMillan, *Science* **2008,** *322,* 77-80.

[6] J.W. Tucker, J.M.R. Narayanam, S.W. Krabbe, C.R.J. Stephenson, *Org. Lett.* **2010,** *12(2),* 368-371.

[7] A.G. Condie, J.C. González-Gómez and C.R.J. Stephenson, *J. Am. Chem. Soc.* **2010,** *132,* 1464-1465.

[8] M. Neumann, S. Füldner, B. König, K. Zeitler, *Angew. Chem.* **2010,** *accepted.*

[9] G. Nagasubramanian, B.L. Wheeler, BA.J. Bard, *Journal of the Electrochemical Society* **1983,** *130,* 1680-1688.

[10] R. Lechner, B. König, *Synthesis* **2010,** *10,* 1712-1718.

[11] H. Kisch, *Adv. Photochem.* **2001,** *62,* 93-143.

[12] F. Fini, L. Bernardi, R. P. Herrera, D. Pettersen, A. Ricci, V. Sgarzani, *Adv. Synth. Catal.* **2006,** *348,* 2043-2046.

[13] G. Manickam, G. Sundararajan, *Tetrahedron: Asymmetry* **1999,** *10,* 2913-2925.

[14] A. L. Tillman, D. J. Dixon, *Org. Biomol. Chem.* **2007,** *5,* 606-609.

[15] X.-M. Zhang, F. G. Bordwell, M. Van Der Puy, H. E. Fried, *J. Org. Chem.* **1993,** *58,* 3060-3066.

[16] Y. Xu, C. H. Langford, *J. Photochem. Photobiol. A: Chem.* **2000,** *133,* 67-71.

[17] A. Kumar, N. Mathur, *J. Colloid. Interface Sci.* **2006,** *300,* 244-252.

[18] R. F. P. M. Moreira, T. P. Sauer, L. Casaril, E. Humeres, *J. Appl. Electrochem.* **2005,** *35,* 821-829.

[19] S. Füldner, R. Mild, H.I. Siegmund, J.A. Schroeder, M. Gruber, B. König, *Green Chem.* **2010,** *12,* 400-406.

[20] D. Srinivas, R. Srivastava, P. Ratnasamy, *Catal. Today* **2004,** *196,* 127-133.

[21] B. J. Flower, R. Gautreau-Service, P. G. Jessop, *Adv. Synth. Catal.* **2008,** *350,* 2947-2958.

[22] B. M. Trost, L. S. Melvin Jr., *J. Am. Chem. Soc.* **1976,** *98,* 1204-1212.

3.5 Supporting information

3.5.1 Exemplary GC analyses of photoreductions

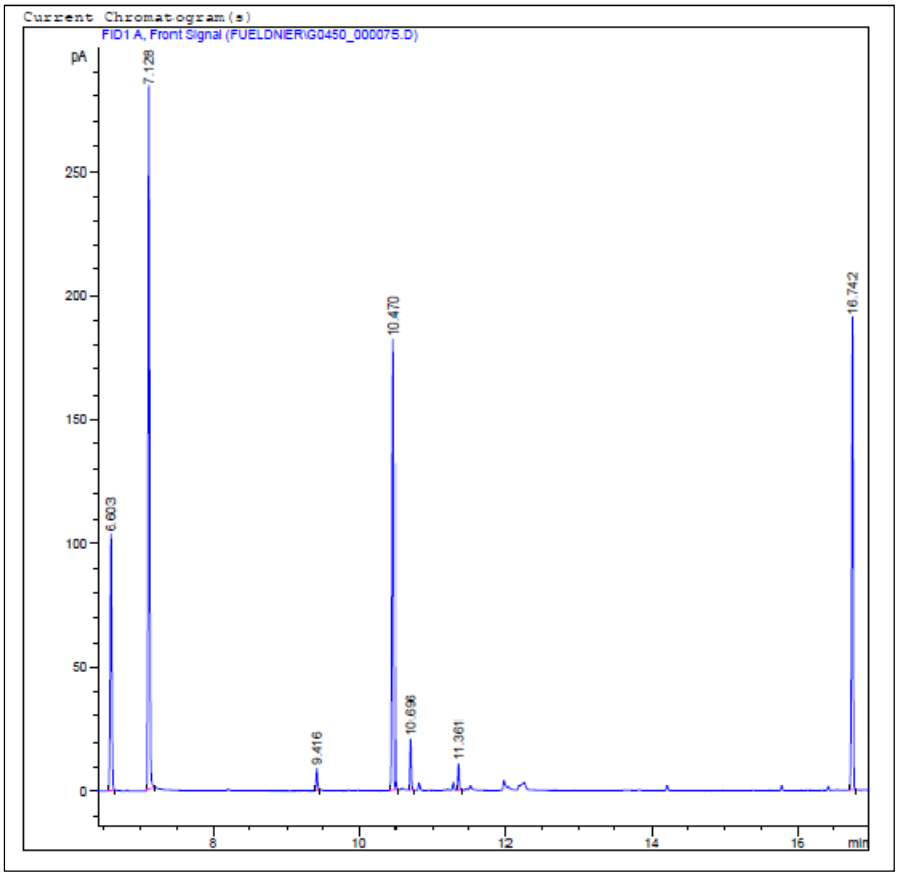

GC-chromatogram of the α-alkylation of octanal with 2-bromo diethylmalonate after 10 h of irradiation with LED 400 nm at - 10 °C: chlorobenzene t = 6.60 min, 2,6-lutidine t = 7.13 min, hydrocinnamaldehyde t = 10.47 min, 2-bromo diethylmalonate t = 11.36 min and (*R*)-Diethyl 2-(1-oxo-3-phenylpropan-2-yl)malonate t = 16.74 min.

3.5.1 Exemplary NMR-spectra of isolated compounds

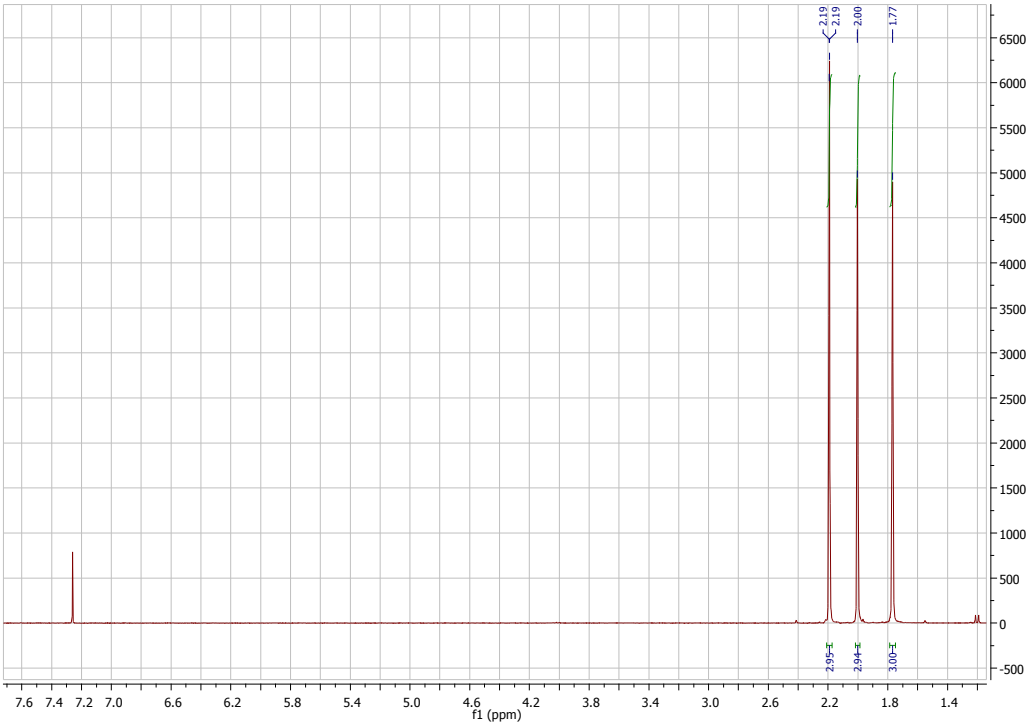

^{1}H-NMR-spectrum of *cycl*-isopropylidene 1-bromo-methylmalonate **1**.

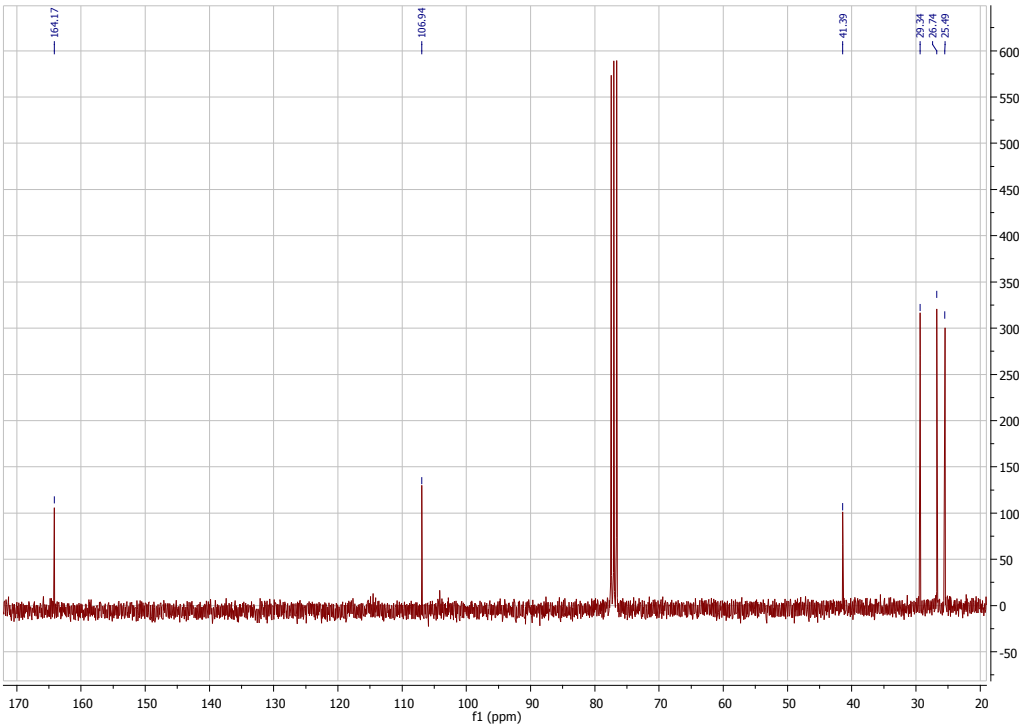

^{13}C-NMR-spectrum of *cycl*-isopropylidene 1-bromo-methylmalonate **1**.

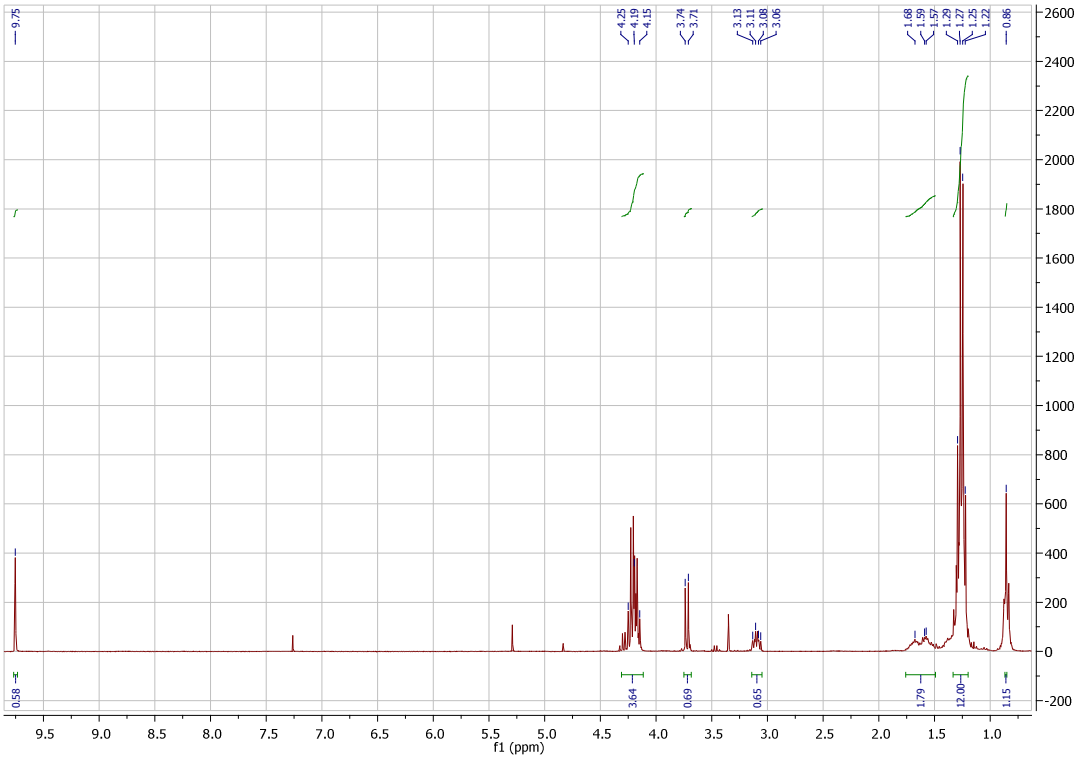

[1]H-NMR-spectrum of (*R*)-diethyl 2-(1-oxooctan-2-yl)malonate **2**.

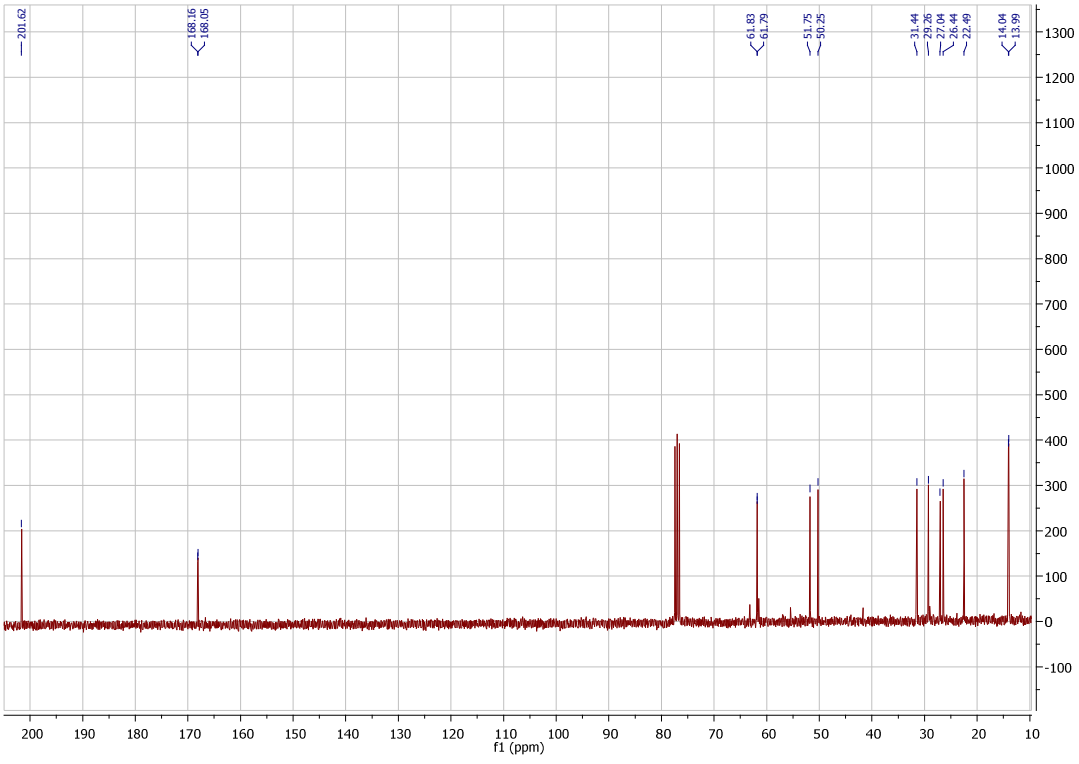

[13]C-NMR-spectrum of (*R*)-diethyl 2-(1-oxooctan-2-yl)malonate **2**.

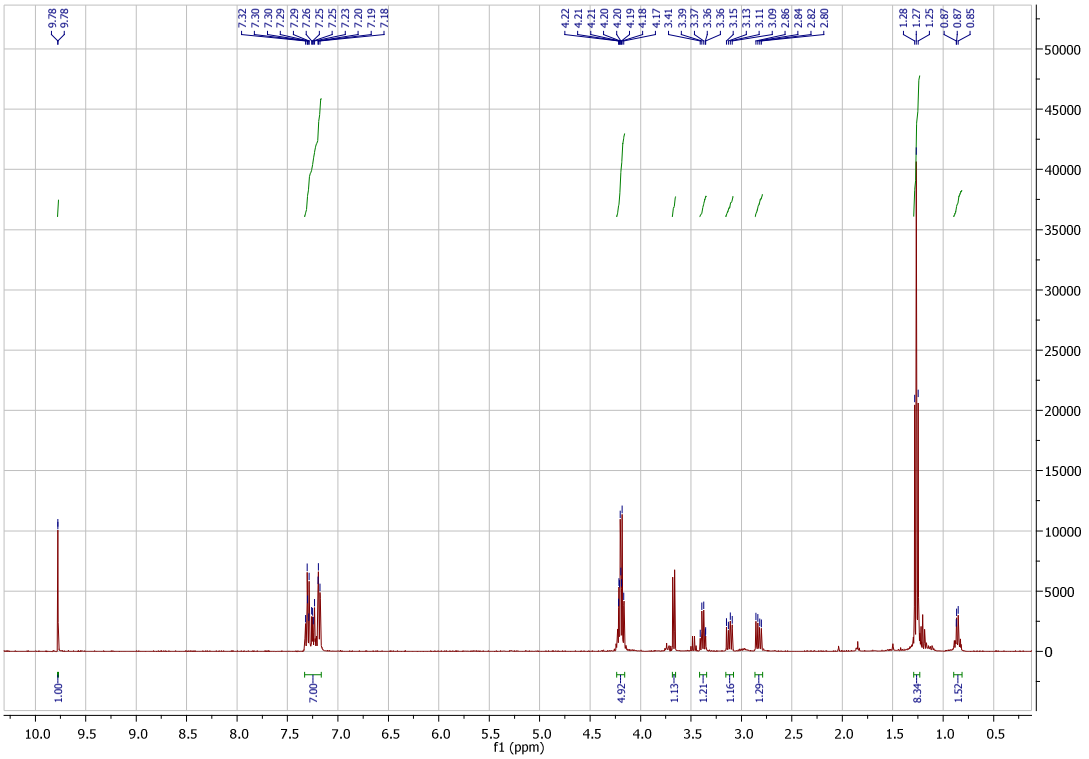

^{1}H-NMR-spectrum of (*R*)-Diethyl 2-(1-oxo-3-phenylpropan-2-yl)malonate **3**.

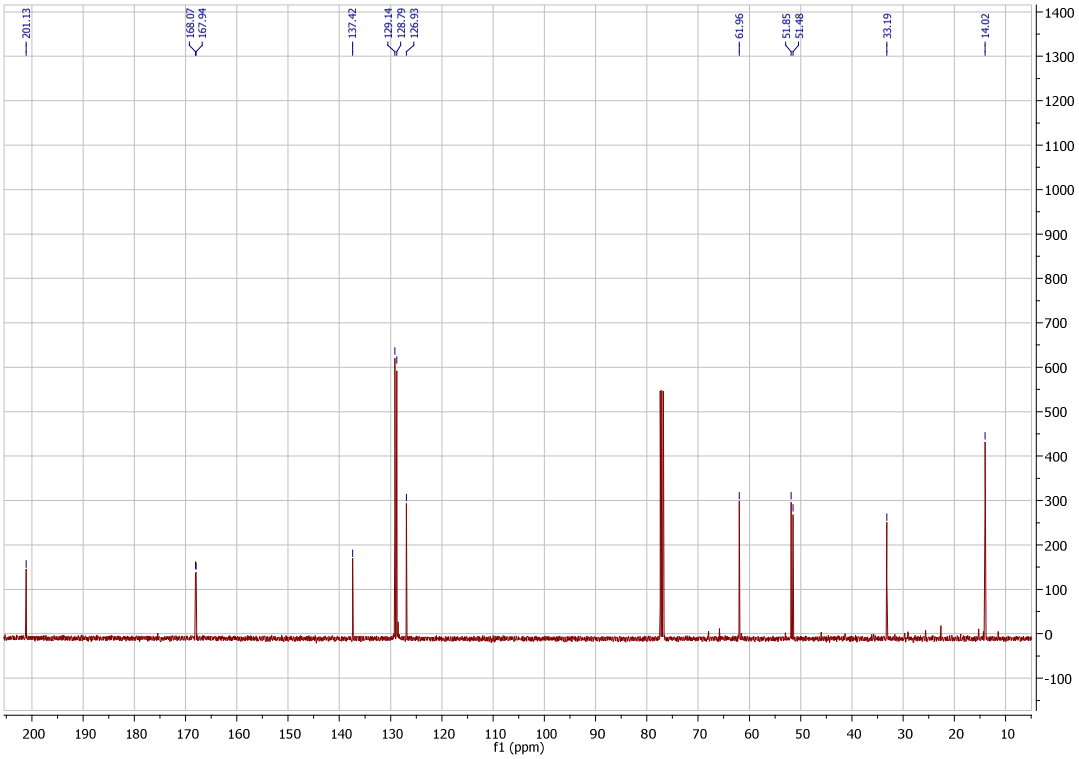

^{13}C-NMR-spectrum of (*R*)-Diethyl 2-(1-oxo-3-phenylpropan-2-yl)malonate **3**.

4 Summary

The first part of this dissertation (chapter 1) deals with the green-light-induced reduction of nitrobenzenes by using dye-sensitized TiO_2 and transition metal nanoparticles (chapter 1.2) or nanomolar amounts of urea derivatives (chapter 1.3). In the case of transition metal nanoparticles, clusters were found by TEM and dihydrogen gas was detected by GC-MS. The dependence of the conversion on the amount of initially used transition metal salt has been explained by the formation of these nano clusters of an average size of 20 nm, which show highest catalytic activity. Urea and urea derivatives can replace transition metal ions and lead to full conversions in case of the reduction of nitrobenzene derivatives to their anilines, too. Absence of detectable dihydrogen gas, linear kinetics and deuterated triethanolamine indicate that the acceleration of the protonation coupled with each electron transfer step is the origin of the catalytic effect.
For the first time, nitrobenzene derivatives have been cleanly reduced to their anilines via green light and dye-sensitized TiO_2.

The second part of this work (chapter 2) presents the blue-light-induced selective reductions of nitrobenzene and derivatives by semiconductors of the general formula $PbBiO_2X$ (X = Br, Cl). These materials have been known for the oxidative photodegradation of organic dyes, such as methylene blue or methyl orange by irradiating with high intensive light < 440 nm. We observed the selective and clean photoreduction of nitro arenes to their anilines by irradiating these semiconductors with visible light (440 nm / ± 10) and less power (3 Watt LEDs). The difference and role of Bi^{3+} and Sb^{3+} in the $Pb\mathit{Pn}O_2X$ structures and the photocatalytic activity dependence of $PbBiO_2X$ of their anions Cl^-, Br^- and I^- could be explained by electronic quenching and structure effects. These materials are useful catalysts in selective photoreductions of nitro groups with light of the visible solar spectrum.

The last part of this thesis (chapter 3) summarizes α-alkylations of aldehydes using the MacMillan-organocatalyst and unmodified TiO_2 (Degussa, Anastas/ Rutil 80/20) as photocatalyst. Preliminary, product yields of 87 % and stereoselectivities of up to 85 % *ee* have been obtained for this semiconductor mediated enantioselective *C-C* bond formations under optimized reaction conditions. However, surface-interaction-effects of TiO_2 and substrates currently limit the application to diethylmalonate's addition. Mono ketones and

mono esters are not successfully converted. Furtherinvestigations are necessary to understand electronic and steric effects of radical precursors and TiO_2 interactions.

5 Zusammenfassung

Der erste Teil dieser Dissertation (Kapitel 1) behandelt selektive photokatalysierte Reduktionen von Nitrobenzolderivaten zu ihren entsprechenden Anilinen. Farbstoffsensibilisertes TiO_2 (Degussa P25) bildet den eigentlichen Photokatalysator, der unter Bestrahlung von grünem Licht (LEDs 530 nm ± 10 nm) oder Sonnenlicht und Additiven Nitrobenzolderivate zu ihren Anilinen reduziert. Zum einen sind als Additive Übergansmetallionen in kleinen Mengen von 10^{-2} bis 10^{-4} mol% hinzugegeben worden, die unter Bestrahlung in Lösung Metallcluster der Größe von etwa 20 nm bilden und Protonen zu Wasserstoff reduzieren (Kapitel 1.2). Dieser bildet die Elektronen- und Protonenquelle für die Nitrobenzolreduktion. Zum anderen wurden winzige Mengen von 10^{-4} bis 10^{-6} mol% an Harnstoffderivaten hinzugegeben, die die gleiche Selektivität und Vollständigkeit in den Reduktionen von Nitrobenzolderivaten zeigten (Kapitel 1.3). Fehlender Wasserstoff, ein linearer kinetischer Reaktionsverlauf und Deuterierungsexperimente zeigten, dass Harnstoff und seine Derivate nicht die Elektronenübertragung, sondern den Protonentransport der entsprechenden Intermediate katalysieren.

Der zweite Teil dieser Dissertation (Kapitel 2) befasst sich mit selektiven chemischen Reaktionen von Halbleitern der Zusammensetzung $PbPnO_2X$ (*Pn* = Bi, Sb; *X* = Cl, Br, I), welche bekannterweise unter Bestrahlung mit sehr intensiven Lichtquellen Farbstoffe wie Methylorange oxidativ und unselektiv zersetzen. Wir konnten erstmalig zeigen, dass gezielte selektive Reduktionen von Nitrobenzolderivaten zu ihren Anilinen durch Wasserstoffentwicklung während der Bestrahlung dieser Halbleiter möglich sind und dass kristallstrukturbedingt Bi^{3+} katalytisch aktiv ist und Sb^{3+} nicht. Die Unterschiede zwischen $PbBiO_2X$ (*X* = Cl, Br) und $PbBiO_2I$ in ihren photokatalytischen Aktivitäten konnten ebenfalls durch Ursachen in ihren Kristallstrukturen und elektronische Löschungsversuche mit Iodid erklärt werden.

Der letzte Teil dieser Arbeit (Teil 3) beschäftigt sich mit heterogenen Organophotokatalysen, wobei α-Alkylierungen von Aldehyden mit einem MacMillan-Organokatalysator und TiO_2 (Degussa P25, Anastas/ Rutil 80/20) als Photokatalysator untersucht wurden. Erstmalig wurden mit einem heterogenen Organophotokatalysesystem und sichtbarem Licht hohe Ausbeuten von 87 % und *ee*-Werte von 85 % bei der Substitution von 2-Bromdiethylmalonat erzielt, dennoch erwies sich dieses System als sehr substratbeschränkt. Durch Untersuchungen

weiterer Monoketone und -ester wurden Hinweise erhalten, dass Radikalstabilitäten eine untergeordnete Rolle spielen, aber die Wechselwirkungen der Substrate mit der TiO_2-Oberfläche, die durch Moleküle mit zwei Carbonylgruppen ausgeprägter sind, entscheidend sind.

Publications and Articles

Selective Photocatalytic Reductions of Nitrobenzene Derivatives via $PbBiO_2X$ and Blue Light, S. Füldner, P. Pohla, H. Bartling, S. Dankesreiter, R. Stadler, M. Gruber, A. Pfitzner, B. König, *Green Chem.* **2010,** *submitted.*

Enhanced Photocatalytic Activity of Dye-modified Titaniumdioxide Particles at the Presence of Urea Derivatives, S. Füldner, T. Mitkina, T. Trottmann, A. Frimberger, M. Gruber, B. König, J. *Photochem. Photobiol. A: Chemistry* **2010,** *submitted.*

Metal-Free, Visible Light Cooperative Asymmetric Organophotoredox Catalysis, M. Neumann, S. Füldner, B. König, K. Zeitler, *Angew. Chem.* **2010,** *DOI: 10.1002/anie.201002992.*

NACHHALTIGE CHEMIE: 14TH ANNUAL ACS GREEN CHEMISTRY AND ENGINEERING CONFERENCE, S. Füldner, S. Hübschmann. U. Hintermayr, Y. Neumann, A. Boddien, *Nachrichten aus der Chemie* **2010,** *9,* 956.

Green-Light Photocatalytic Reductions using Dye-Sensitized TiO_2 and Transition Metal Nanoparticles, S. Füldner, R. Mild, H.I. Siegmund, J.A. Schroeder, M. Gruber, B. König, *Green Chemistry* **2010,** *12(3),* 400-406.

Supramolecular Catalysis, S. Füldner, B. König, *ChemSusChem* **2009,** *2,* 185-187.

Microwave-Assisted Synthesis of 1,5- and 2,6-linked Naphthylene-Based Ladder Polymers, B.S. Nehls, S. Füldner, T. Farell, U. Scherf, *Macromolecules* **2005,** *38,* 687-694.

Semiconducting Polymers via Microwave-Assisted Suzuki and Stille Crosscoupling Reactions, B.S. Nehls, U. Asawapirom, S. Füldner, E. Preis, T. Farell, U. Scherf, *Adv. Funct. Mater.* **2004,** *14,* 352-356.

Conferences and Posters

09/2010	22th Lecture Conference of the GDCh-division Photochemistry, Erlangen
06/2010	Annual 14th Green Chemistry & Engineering Conference in Washington D.C.
04/2010	Chemie-Cluster Bayern *Zukünftige Rohstoffe in der chemischen Industrie*, Wissenschaftszentrum Straubing
03/2008	Chemie-Cluster Bayern, Universität Regensburg
02/2007	*Glycan*, Glykopeptid-Tagung, Charité Berlin
06/2003	*Koordinationschemie des 1,12-Diazaperylens,* Tag der Chemie, Humboldt-Universität Berlin.

Talks

04/2010	*Heterogeneous Photocatalyst for Reactions with Blue and Green Light*, Kick-off Meeting *Chemical Photocatalysis - GRK 1626,* Wildbach Kreuth.
12/2009	*Sunny Perspectives - Heterogeneous Photocatalysis*, Vortrag Weihnachts-kolloquium am Institut für Organische Chemie, Universität Regensburg.
07/2009	*Heterogene Photokatalysatoren für Umsetzungen mit blauem und grünem Licht,* Antrag auf das Graduiertenkolleg *Chemische Photokatalyse - GRK 1626*, Universität Regensburg.

Curriculum vitae

Stefan Füldner

*21.08.1979, Ludwigsfelde (Brandenburg/ Germany)

Education

09/2007 - 12/2010	Dissertation: "Blue- and Green-Light-Induced Reductions and *C*-*C* Bond Formations with TiO_2 and $PbPbO_2X$", University of Regensburg
11/2006 - 06/2007	Diploma thesis: "Darstellung quaternärer *C*-*2*-verknüpfter Glykoaminosäurederivate durch [3+2]-Cycloaddition an *glyco*-Isoxazolin-*N*-oxiden", University of Potsdam
10/2002 - 10/2006	Studies of Chemistry, University of Potsdam
08/1999 - 06/2002	Apprenticeship Laboratory Assistant, University of Potsdam

Research Experiences

03/2005 - 07/2006	Studentische Hilfskraft at the Institute of Organic Chemistry, University of Potsdam
04/2004 - 07/2004	Studentische Hilfskraft at the Institute of Kolloid- und Grenzflächenforschung, Max-Planck-Institute of Golm/ Potsdam
10/2002 - 03/2004	Studentische Hilfskraft at the Institute of Inorganic Chemistry, University of Potsdam

Teaching Experiences

10/2004 - 07/2007	Teaching assistant in subjects Organic and Physical Chemistry for students of Biochemistry, Chemistry and Geoecology

PhD Scholarships

04/2010 - 10/2010	*Graduate School 1626* - Chemical Photocatalysis
04/2008 - 03/2010	*Bayerische Eliteförderung*

Honors

06/2010	Scholarship of the GDCh for the ACS 14th Annual Green Chemistry & Engineering Conference in Washington D.C.
09/2010	"Photokatalytisch" by Julia Nistor, Acryl on hard fiber 120 x 90 cm, opening picture for the conference at the university of Regensburg

Engagements

05/2008	Member of the association “Drugstop - Drogenhilfe Regensburg e.V.”
01/2008	Member of the association “Rauhreif - Arbeitsgemeinschaft gegen sexuellen Missbrauch e.V.”
01/2003	Member of the GDCh and Jungchemikerforum